Journal of Drug Delivery Science and Technology 127 (2027) 108853

Contents lists available at ScienceDirect

Journal of Drug Delivery Science and Technology

journal homepage: www.elsevier.com/locate/jddst

# Quaternary ammonium salts derived from Vitamin B as multifunctional (anti-inflammatory and antimicrobial) therapeutic agents

Adriana Olejniczak [a], Daniela Gwiazdowska [b], Krzysztof Juś [b], Anna Olejnik [d], Mara G. Freire [c], Michał Niemczak [a,*]

[a] Faculty of Chemical Technology, Poznan University of Technology, Berdychowo 4, Poznan, 61-131, Poland
[b] Department of Natural Science and Quality Assurance, Poznan University of Economics and Business, al. Niepodległosci 10, Poznan, 60-967, Poland
[c] CICECO-Aveiro Institute of Materials, Chemistry Department, University of Aveiro, Aveiro, 3810-193, Portugal
[d] Department of Biotechnology and Food Microbiology, Poznan University of Life Sciences, 48 Wojska Polskiego St., Poznan, 60-627, Poland

ARTICLE INFO

*Keywords:*
Quaternary ammonium salts
B vitamins
Anti-inflammatory
Egg albumin denaturation
Antibacterial
Active pharmaceutical ingredient

ABSTRACT

Antimicrobial resistance is a current critical challenge, requiring the urgent development of new, effective broad-spectrum antimicrobials. To tackle this challenge, in this work, naturally occurring B vitamins, viz. nicotinamide, nicotinic acid and *p*-aminobenzoic acid, were used as precursors of both the cation and anion to design novel ionic liquids (ILs) in the form of quaternary ammonium salts (QASs). These combinations allowed for the development of multifunctional (anti-inflammatory and antimicrobial) agents targeting oral administration. The QASs were synthesized, characterized, and evaluated for the therapeutic potential as well as mechanism of the antimicrobial activity. Mixtures and cocrystals of the starting materials were also investigated for comparison purposes. Salts with the *p*-aminobenzoate anion showed excellent anti-inflammatory activity, inhibiting albumin denaturation by up to 54%, remarkably outperforming diclofenac sodium at its peak plasma concentration. Both albumin-based and *in silico* COX-2 studies further indicated that increasing the alkyl chain length significantly enhances the compounds' efficacy. Antimicrobial tests showed that QASs were up to 250 times more effective than their non-ionic analogues. Moreover, the salts with the highest bactericidal activity completely inhibited biofilm growth against *S. aureus* and *P. aeruginosa*. Solubility studies under simulated gastrointestinal pH showed higher solubility of QASs, up to 100-fold, compared to the non-ionic forms. Cytotoxicity assay using human normal small intestinal cells (HIEC-6) revealed that even the most potent vitamin B analogues, were approximately ten times less toxic than the widely applied pharmaceutical agent, benzalkonium chloride. Ecotoxicity studies using *A. franciscana* also confirmed their low environmental impact.

## 1. Introduction

In an era of increasing bacterial resistance to antibiotics the need for novel compounds with diverse spectrum of antimicrobial activity is currently considered one of the key challenges of next-generation drug development[1]. Novel strategies in infection treatment should lead not only to combating microorganisms, but also alleviate side effects of their action such as inflammation, which often delays the healing process. Therefore, particular attention should be paid to substances with multifunctional biological activity, which not only eliminate pathogens, but also show effects that support recovery processes and reduce inflammation. Various studies unambiguously indicate that compounds with simultaneous antimicrobial and anti-inflammatory activity can help to shorten recovery time and reduce the risk of complications, allowing for a more comprehensive fight against infection[2]. On the other hand, more hydrophobic and neutral drugs tend to display low water solubility, and consequently low bioavailability. This drawback can be overcome by converting these drugs into the form of salts, increasing thus their water solubility. In this context, properly designed quaternary ammonium salts (QASs) that contain Active Pharmaceutical Ingredients (APIs) may provide modern therapeutic systems with improved efficacy, dual function, and better stability than conventional drugs[3–5]. It is also worth noting that numerous QASs, such as cetylpyridinium chloride (CPC) and benzalkonium chloride (BAC), have long been used in pharmaceuticals and consumer products. These compounds are commonly used in lozenges for sore throats, disinfectants, eye drops

* Corresponding author. Poznan University of Technology, Berdychowo 4, Poznan, 61-131, Poland.
*E-mail address:* michal.niemczak@put.poznan.pl (M. Niemczak).

https://doi.org/10.1016/j.jddst.2026.108853
Received 24 February 2026; Received in revised form 11 August 2026; Accepted 27 August 2026
Available online 28 August 2026

and many other applications (Table S1 in Supporting Information). It should be emphasized that BAC, despite its well-documented hemolytic and cytotoxic effects, also reported in numerous studies on surfactant activity, is still widely used in medical formulations. This fact underscores the relevance of ongoing efforts to identify QASs with improved safety profiles and comparable efficacy.

Transformation of APIs into salts is the preferred method for increasing their solubility and bioavailability, which may also improve other physicochemical and biopharmaceutical properties of the respective drugs. The limited solubility of therapeutic substances, especially in the case of oral drugs - one of the most common routes of administration - hinders their absorption and reduces their effectiveness. Since the bioavailability of a drug depends, among others, on its solubility in body fluids, this is a key factor affecting the effectiveness of a therapy. This is the main reason why nearly half of the drugs currently in use are in the form of salts[6,7]. One approach to converting drugs into a salt is their transformation into an ionic liquid (IL) or organic salts with low melting temperature to surpass the melting enthalpy barrier. While the transport of anions and cations is well understood, challenges remain, prompting researchers to search for new combinations of ions and investigate their potential behavior in the body. For instance, gliclazide tetrabutylphosphonium IL demonstrated improved solubility of gliclazide after IL formation, with a 50-fold increase in water solubility. However, this modification resulted in reduced permeability, as evidenced by *in vitro* studies performed with gastrointestinal artificial membrane permeability tests[8]. Additionally, *in silico* studies on the IL constituted by ions derived from caprolactam and salicylic acid revealed favorable properties (pharmacokinetic and toxicity profile) in comparison to common orally administered drugs[9]. Remarkably, oral administration of the drug in its IL form (proline ethyl ester methotrexate) resulted in almost 5-fold higher bioavailability compared to its sodium salt, highlighting its potential in the improvement of drug delivery[10].

Vitamin $B_{10}$, *p*-aminobenzoic acid (PABA), exhibits significant structural versatility, particularly due to its ability to undergo substitutions at both the amino and carboxyl groups, enabling the design of tailored bioactive derivatives[11,12]. This unique feature makes PABA a valuable building block in pharmaceutical formulations. In a database of 12,111 commercial drugs, PABA is incorporated as a structural component in 1.5% of them[13]. Notably, these pharmaceuticals exhibit a wide range of therapeutic applications, including antimicrobial, anticancer, and anti-inflammatory effects, depending on the derivatization strategy[13,14]. Another B vitamin, vitamin $B_3$, exists in two forms: nicotinamide (NA) and nicotinic acid (NIC), both of which play a critical role in enzymatic reactions, supporting regenerative and immune processes. Beyond its fundamental biological roles, it also exhibits antibacterial activity, making it a promising candidate for anti-infective therapies[15]. The anti-inflammatory properties of vitamin $B_3$ are well-documented, making it a particularly valuable component in promoting optimal health and maintaining homeostasis[16,17]. Furthermore, NA, PABA and NIC are widely used in dietary supplements and dermatological preparations, where they support skin regeneration, metabolism, and reduce inflammation. In addition to their use in drug formulations, these properties make them an attractive basis for their use as pharmaceuticals *per se*. Based on this possibility, structural modifications of NA, NIC and PABA into ionic derivatives have gained particular interest. These QASs have been explored, among others, for applications in targeted cancer therapy, dermatology, and in the treatment of type A influenza[18–21] Nevertheless, a direct combination of NA, PABA, and NIC in the form of ionic pairs has yet to be investigated.

In this work, we focused on exploring the potential of different forms of vitamin B as naturally derived, multifunctional APIs. Our aim was to elucidate their individual contributions to antimicrobial and inflammation-related activities, and to preliminarily assess their potential depending on the form used (organic salt, mixture, or cocrystal). A systematic structure–activity relationship (SAR) analysis was performed to evaluate the influence of alkyl chain length and counterion type on the physicochemical and biological properties. This approach not only opens the door to innovative new drugs with improved efficacy and targeting several treatments but also enables the use of widely available substances with low toxicity. We focused also on determining the threshold at which increasing antimicrobial activity, typical for amphiphilic QASs, begins to compromise cellular tolerance due to enhanced interactions with biological membranes, potentially limiting oral drug applicability. This approach strengthens mechanistic understanding and supports rational selection of promising candidates, highlighting multifunctionality as a simple yet effective strategy for developing safer alternatives to conventional QAS-based agents.

## 2. Materials and methods

### 2.1. Materials

1-Bromohexane, (99%), 1-bromooctane (99%), 1-bromodecane (98%), 1-bromododecane (97%), octan-1-ol (99%), nicotinamide (98%), nicotinic acid (98%) and *p*-aminobenzoic acid (99%) were purchased from Sigma-Aldrich (Saint Louis, MO, USA). All solvents (methanol (99.8%), ethanol (96%), acetonitrile (99%), acetone (99%)), *n*-propanol (99.5%), potassium hydroxide (99%), diclofenac sodium (DCF-Na) and egg albumin powder were obtained from Avantor (Gliwice, Poland) and used without further purification. Phosphate-buffered saline (PBS) solution was prepared by dissolving 8.0 g of NaCl, 0.2 g of KCl, 1.42 g of $Na_2HPO_4$, and 0.24 g of $KH_2PO_4$ in 1 L of deionized water. Its pH was adjusted to 7.4 using HCl solution. Simulated gastric fluid (SGF) without pepsin consists of 0.2% (w/v) sodium chloride and 0.7% (v/v) concentrated HCl. Artificial sea water was prepared by dissolving 26.4 g NaCl, 0.84 g KCl, 1.67 g $CaCl_2{\cdot}2H_2O$, 4.60 g $MgCl_2{\cdot}6H_2O$, 5.58 g $MgSO_4{\cdot}7H_2O$, 0.17 g $NaHCO_3$, 0.03 g $H_3BO_3$ in 1 L of deionized water. Deionized water with a conductivity of $<0.1$ μS $cm^{-1}$, from Hydrolab HLP Smart 1000 demineralizer (Straszyn, Poland) was used. The microbiological broth media included Nutrient Broth, Mueller-Hinton Broth, TSB and BHI Broth for bacteria and PDB Broth for yeast purchased in BioMaxima (Poland) were used.

### 2.2. General

$^1$H NMR spectra were recorded on a Varian VNMR-S 400 MHz spectrometer (Palo Alto, USA) with TMS as the internal standard. $^{13}$C NMR spectra were obtained with the same instrument at 100 MHz. The FTIR spectra were collected by using a EasyMax 102 semi-automated system (Mettler Toledo, Switzerland) connected to a ReactIR iC15 (Mettler Toledo, Switzerland) probe equipped with an MCT detector and a 9.5 mm AgX probe with a diamond tip. The data were sampled from 3000 to 650 $cm^{-1}$ with 8 $cm^{-1}$ resolution and processed by iCIR 4.3 software. The water content in all obtained products was measured with a TitroLine 7500 KF trace apparatus (SI Analytics, Germany) using the Karl Fischer titration method. The water content in the compounds was determined by analyzing their solutions in dehydrated methanol with a known water content. The melting points of the compounds obtained were analyzed *via* an MP90 Melting Point System (Mettler Toledo, Switzerland). The precision of the measurements was ensured by calibration of the apparatus using certified reference substances.

### 2.3. Synthesis

Initially, nicotinic acid (NIC) and *p*-aminobenzoic acid (PABA) were neutralized with stoichiometric amounts of potassium hydroxide in dehydrated methanol in a EasyMax 102 semi-automated system (Mettler Toledo, Switzerland) equipped with a pH-meter with calibrated glass electrode. Then, the solvent was evaporated using a rotary vacuum evaporator. The obtained potassium nicotinate ([K][NIC]) and potassium *p*-aminobenzoate ([K][PABA]) were dried in a vacuum oven at 25 °C for 24 h. Appropriate *N*-alkylnicotinamide bromides were

obtained *via* quaternization of nicotinamide (NA) with the corresponding alkyl bromide in prOH, according to the methodology described previously by Stachowiak et al.[22].

### 2.3.1. Preparation of N-alkylnicotinamide nicotinates (1–4)

0.01 mol of an appropriate *N*-alkylnicotinamide bromide (**P1**–**P4**) was dissolved in 10 mL of dehydrated methanol in round-bottomed flask equipped with a mechanical stirrer. Next, [K][NIC] dissolved in 10 mL of dehydrated methanol, was added with a 2% of molar excess (0.0102 mol) to perform the ion exchange reaction (Fig. 1A). The reaction mixture was stirred at 40 °C for 15 min and then cooled to 0 °C. As a result of anion exchange, a sediment of potassium bromide precipitated from the post-reaction mixture. Subsequently, the inorganic salt was filtered off and the solvent was evaporated from the filtrate. The obtained products were additionally purified by the addition of a small portion (10–15 mL) of acetone, which enabled to isolate the residues of inorganic impurities and excess reactant through vacuum filtration. After evaporation of acetone, the obtained products were dried in a vacuum oven under reduced pressure (1–2 mbar) at 25 °C for 24 h. The reaction yields were calculated based on the mass of the isolated products after drying, taking into account both synthetic steps (quaternization and ion-exchange). Details regarding the syntheses and the obtained compounds are listed in Table S2 (in Supporting Information).

### 2.3.2. Preparation of N-alkylnicotinamide p-aminobenzoates (5–8)

0.01 mol of an appropriate *N*-alkylnicotinamide bromide was dissolved in 10 mL of dehydrated methanol in round-bottomed flask equipped with a mechanical stirrer. Next, [K][PABA] dissolved in 10 mL of methanol, was added with a 2% of molar excess (0.0102 mol) to perform the ion exchange reaction (Fig. 1A). The reaction mixture was stirred at 40 °C for 15 min and then cooled to 0 °C. As a result of anion exchange, a sediment of potassium bromide precipitated from the post-reaction mixture. Subsequently, the inorganic salt was filtered off and the solvent was evaporated from the filtrate. The obtained products were additionally purified by the addition of mixture of hot acetone and methanol (20-25 mL) in proportion 20:1 followed by vacuum filtration. This action allowed to isolate the desired product, which precipitated from cooling filtrate and was separated by vacuum filtration. Finally, the obtained compounds were dried in a vacuum oven under reduced pressure (1–2 mbar) at 25 °C for 24 h. The reaction yields were calculated based on the mass of the isolated products after drying, taking into account both synthetic steps (quaternization and ion-exchange). Details regarding the syntheses and the obtained compounds are listed in Table S2 (in Supporting Information).

### 2.3.3. Preparation of [NA][NIC] mixture and [NA][PABA] cocrystal

The preparation of nicotinamide (NA) and nicotinic acid (NIC) mixture was accomplished by mixing the appropriate amount of nicotinamide (0.01 mol) with the equimolar amount of nicotinic acid in 25 mL of methanol, and stirred for 2 h at room temperature. The remaining solvent was then removed using a rotary evaporator. The same methodology was applied for synthesis of nicotinamide (NA) and *p*-aminobenzoic acid (PABA) cocrystal (Fig. 1B). Finally, **[NA] [NIC]** and **[NA] [PABA]** were dried in a vacuum oven under reduced pressure

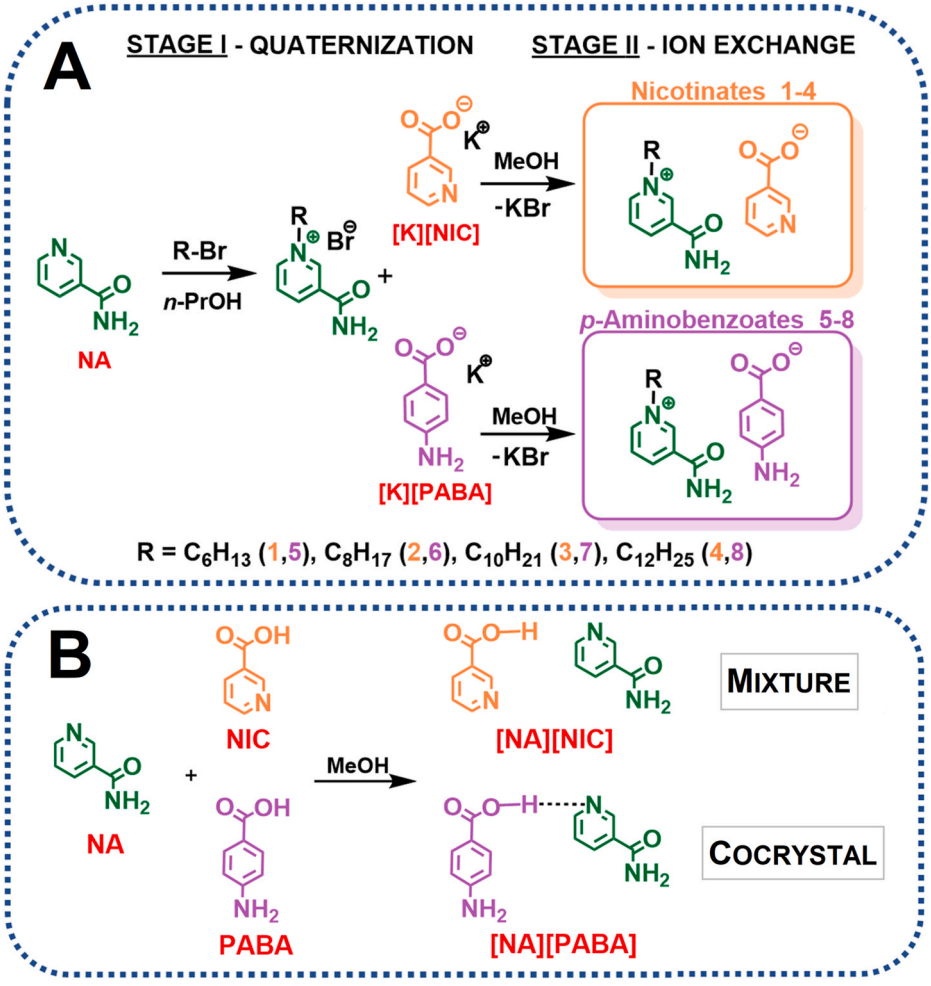


**Fig. 1.** Synthesis of *N*-alkylnicotinamide nicotinates **(1-4)** and *N*-alkylnicotinamide *p*-aminobenzoates **(5–8)** (**A**); preparation of nicotinamide and nicotinic acid mixture (**[NA] [NIC]**) and nicotinamide and *p*-aminobenzoic acid (**[NA] [PABA]**) cocrystal (**B**).

(1–2 mbar) at 25 °C for 24 h. The yields **[NA] [NIC]** and **[NA] [PABA]** were calculated based on the mass of the solids obtained after drying (Details are listed in Table S2 in Supporting Information).

### 2.4. Determination of purity

#### 2.4.1. Two phase titration technique

The content of cationic active substances (products **1**–**8**) was determined by direct two-phase titration according to EN ISO 2871-1:2010. The method is based on titration of the respective quaternary ammonium salts in a water–chloroform biphasic system using a standard sodium dodecyl sulfate(VI) solution and a mixed indicator. Dimidium bromide (CAS No. 518-67-2) was used for the determination of cationic active substances, while sulfan blue (CAS No. 129-17-9) was employed for anionic species. The results are expressed as the mean values from three independent determinations.

#### 2.4.2. LC/MS/TOF analysis

The purity of products **1**–**8** was analyzed in 3 replicates using liquid chromatography/time-of-flight/mass spectrometry (LC/MS/TOF). The analysis was performed using a 1290 Infinity UHPLC system coupled with a 6546 Quadrupole Time-of-Flight Mass Spectrometer with a Dual AJS ESI source (Agilent Technologies, Santa Clara). Chromatographic separation was performed using a ZORBAX RRHD Eclipse Plus C18 column 2.1 × 50 mm, 1.8 μm (Agilent Technologies, Santa Clara), which was maintained at a temperature of 35 °C. The mobile phase consisted of solvent A (water with 0.1% formic acid) and solvent B (acetonitrile). The injection volume was 3 μL. Compound detection was carried out in positive electrospray ionization mode using the Dual Agilent Jet Stream source. Parameters were set as follows: drying gas temperature, 320 °C; drying gas flow, 10 L/min; nebulizer pressure: 45 psi, sheath gas temp: 350 °C, sheath gas flow: 12 L/min, capillary entrance voltage 4000 V, nozzle voltage 0 V. Stock solutions of each compound were prepared by accurately weighing an appropriate amount of substance and dissolving it in water, followed by dilution to obtain the desired mass spectrometric response.

#### 2.4.3. Elemental analysis

The elemental analyses (CHN) were performed by using Elementar Analyser Vario EL III at the Adam Mickiewicz University, Poznan (Poland).

### 2.5. Octanol-water partition coefficient

The octanol-water partition coefficients ($K_{OW}$) of the synthesized products were estimated by the slow-stirring method according to the OECD Test No. 123 guidelines[23]. Measurements were performed using mutually saturated distilled water and 1-octanol in a glass vial containing a magnetic stir bar. First, the synthesized products were dissolved in 1-octanol at chosen concentration (0.01 mol per 1 L of octanol), and then proper amounts of water were added. Subsequently, two duplicate runs were carried out with different solvent ratios: 4 mL of 1-octanol and 2 mL of water (2:1), 4 mL of 1-octanol and 4 mL of water (1:1) and 4 mL of 1-octanol and 8 mL of water (2:1). All were carefully stirred at 150 rpm at constant temperature of 25 °C. After 72 h, all samples were centrifuged and the aqueous and octanolic phases were collected with a syringe. The concentrations of compounds in water were determined using a VWR UV-6300PC spectrophotometer based on calibration curves made previously (at $\lambda_{max}$ = 262–264 nm in the case of nicotinate anion, at $\lambda_{max}$ = 267–269 in the case of *p*-aminobenzoate anion, at $\lambda_{max}$ = 262–263 nm in the case of **[NA] [NIC]** and at $\lambda_{max}$ = 263–289 nm in the case of **[NA] [PABA]**) *vs* concentration for each substance. Two repetitions of each measurement were performed in a specific solvent ratio (1:1, 1:2 and 2:1). Finally, the log $K_{OW}$ was calculated as the average of six results collected for each compound.

### 2.6. Anti-inflammatory potential

#### 2.6.1. Egg albumin denaturation assay

The egg albumin denaturation assay, was performed according to Chaiya et al.[24], with slight modifications that were introduced to simplify the process and improve result reproducibility. The assay was carried out by combining 2 mL of 1% egg albumin solution (from commercially available egg albumin powder), 1 mL of sample solution (**1-8**, **[NA] [NIC]** or **[NA] [PABA]**) or standard (diclofenac sodium) at varying concentrations (1000, 100, 10, 1, 0.1, 0.01, 0.001 and 0.0001 μg/mL) to form a mixture of a total volume of 3 mL. A total volume of 3 mL of the control was obtained by combining 1 mL of phosphate-buffered saline (PBS) and 2 mL of 1% egg albumin solution in 20 mL vials. Then, mixtures were incubated at 90 °C ± 2 °C for 25 min in a MEMMERT UF55 oven, allowing the solutions in the vials to reach a temperature of 37 °C (The temperature increase in the test vials was monitored using a thermocouple). Then, the vials content was allowed to cool down at room temperature. Absorbance of mixture after incubation was measured for each concentration at 660 nm using a VWR UV-6300PC spectrophotometer. Each test was repeated thrice and the mean absorbance was calculated. Percentage of inhibition (INH) of protein was determined (eq. (1)) as a percentage of decrease in absorbance (Abs) compared to control:

$$\mathrm{INH} = \left(\frac{Abs_{control} - Abs_{sample}}{Abs_{control}}\right)\cdot 100\% \quad (1)$$

#### 2.6.2. Structure-based molecular docking with cyclooxygenase-2 (COX-2) enzyme

Molecular docking studies were carried out using the CB-Dock2 online server (https://cadd.labshare.cn/cb-dock2/), which integrates AutoDock Vina as the docking engine and automatically identifies potential binding cavities on the protein surface. The approach applies a structure-based blind docking protocol, allowing unbiased exploration of possible ligand binding sites. The crystal structure of cyclooxygenase-2 (COX-2) was obtained from the Protein Data Bank (PDB ID: 1CVU). The protein structure was preprocessed by removing water molecules, heteroatoms, and non-essential ligands. Polar hydrogen atoms and Gasteiger charges were added automatically during CB-Dock2 preprocessing. For the tested quaternary ammonium salts (QASs **1–8**), individual ions were analyzed separately to evaluate their potential molecular interactions with COX-2. The cationic moieties, as well as the anionic counterparts: nicotinate and *p*-aminobenzoate (PABA), were docked independently. This approach reflects the fact that, in aqueous solution, ions remain freely dissociated and the effective concentrations are well below the critical micelle concentration (CMC), thus minimizing aggregation effects. Additionally, mixture of **[NA] [NIC]** and **[NA] [PABA]** cocrystal were also evaluated separately. Both nicotinamide and the corresponding carboxylic acids were docked as individual ligands to assess their distinct binding profiles and potential interaction sites within the COX-2 active channel. The ligand structures were drawn in ChemBioDraw Ultra, converted to three-dimensional conformations, and energy-minimized prior to docking. All structures were uploaded in PDB format, with protonation states adjusted for physiological pH (7.4). Docking simulations were performed using the default AutoDock Vina parameters within CB-Dock2. For each protein–ligand pair, five potential binding cavities were automatically detected. The output included the predicted binding affinity (Vina score, kcal·mol$^{-1}$), cavity volume (Å$^3$), and the grid box center and size (Å). The lowest-energy binding mode was selected for detailed structural interpretation. Special attention was given to key catalytic residues of COX-2: **R120 (arginine)**, **T385 (tyrosine)**, and **S530 (serine)**; and to additional residues contributing to ligand stabilization and selectivity **S353 (serine), L352 (leucine), V523 (valine)**. Protein–ligand interactions were visualized and analyzed using PyMOL (Schrödinger, LLC). Hydrogen bonding, ionic, π–π stacking, and hydrophobic interactions were examined, with

particular focus on salt-bridge formation between carboxylate groups and positively charged residues (Arg, Lys).

### 2.7. Antimicrobial and antibiofilm properties

#### 2.7.1. MIC and MBC/MFC determination

The antimicrobial activity of the tested compounds was determined in relation to Gram-positive bacteria: *Staphylococcus aureus* ATCC 33862, *Enterococcus faecalis* ATCC 19433, *Listeria monocytogenes* ATCC 19111, *Micrococcus luteus* ATCC 4698, Gram-negative bacteria: *Escherichia coli* ATCC 25922, *Pseudomonas aeruginosa* ATCC 9027, *Serratia marcescens* ATCC 8100, *Moraxella catarrhalis* ATCC 25238, yeasts *Candida albicans* ATCC 10231, *Rhodotorula mucilaginosa* DKK 1001 (PUEB collection). Minimal inhibitory concentration (MIC) and minimal bactericidal/fungicidal concentration (MBC/MFC) of the tested compounds was determined using the microdilution method based on methodology described by Kaczmarek et al.[25] with some modifications. First, a series of two-fold dilutions of the tested substances in the concentration range of 0.49 - 1000 μg/mL were prepared in 96-well microplates in MH broth (for *S. aureus*, *P. aeruginosa* and *E. coli*), MH with 10% TSB (for *S. marcescens*, *M. catarrhalis* and *M. luteus*), MH with 10% BHI (for *L. monocytogenes* and *E. faecalis*), PDB (for *C. albicans*, *C. neoformans* and *R. mucilaginosa*). From 24-h cultures of indicator microorganisms inocula with optical density adjusted to 0.5 McFarland standard suspensions were prepared in broth media. Next, 100 μL of the prepared solutions were added to each well to achieve a final concentration of $10^5$ CFU/ml and the plates were incubated for 24 h at 30 or 37 °C, depending on the indicator microorganism. After incubation the optical density of bacterial and yeast growth was determined at 600 nm using BioTek Epoch 2 microplate reader. The results are expressed as the average of three replicates. The MIC value was defined as the concentration of tested substances, inhibiting the growth of the microorganism by at least 90% whereas 100% of inhibition was defined as minimum bactericidal/fungicidal concentration (MBC/MFC).

#### 2.7.2. Determination of antimicrobial activity by well-diffusion assay

The antimicrobial activity of the tested compounds was evaluated using a well-diffusion assay. Suspensions of selected microorganisms adjusted to 0.5 McFarland standard were spread onto agar media. After solidification of the medium, wells (10 mm in diameter) were prepared using a sterile cork borer, and 100 μL of each compound solution (2.0 mg/mL) was introduced into the wells. The plates were incubated at 37 °C for 24 h. Following incubation, inhibition zone diameters were measured in millimeters. All experiments were performed in triplicate, and the mean values are presented.

#### 2.7.3. Antibiofilm properties

The antibiofilm properties of two selected compounds (**4** and **8**) were tested on biofilm formation by *P. aeruginosa* ATCC 9027 and *S. aureus* ATCC 33862 according to the method described by Gwiazdowska et al.[26] Biofilm formation was carried out according to the modified Somrani method[27] using sterile 48-well flat-bottomed microtiter plates. Standardized bacterial cultures in nutrient broth at a concentration of $10^6$ CFU/ml were introduced into each well in an amount of 150 μl, and then 150 μl of the tested compounds were added to achieve final concentrations of 0.5 MIC and 1 MIC. The prepared plates were incubated for 24 h at 37 °C. Subsequently, the suspension was removed from the wells and rinsed three times with sterile water to remove the residual medium and non-adherent cells. Then, the microtiter plates were air-dried for 2 h, and the biofilm biomass was quantified using the modified crystal violet method developed by O'Toole. 300 μl of 0.1% crystal violet solution was added to the dried biofilm, incubated for 15 min, then the plates were washed with water and dried overnight. Then, 300 μl of 30% acetic acid was added to the wells and left for 10-15 min at room temperature (25 °C ± 1 °C). The solution from each well was transferred to a new microtiter plate, and the optical density was measured at a 550 nm wavelength using a BioTek Epoch 2 microplate reader. As a blank, 30% acetic acid in water was used. All experiments were conducted in triplicate parallel repetitions and the results were expressed as a percentage of inhibition of biofilm formation. The results are presented as the arithmetic mean (±standard deviation) from six parallel replicates. Additionally, one-way analysis of variance (ANOVA) was estimated using Tukey's test with a significance level of $p < 0.05$. For all statistical analyses, the Microsoft Excel® and IBM SPSS Statistics 29 (PS IMAGO PRO 10.0) programs were used.

#### 2.7.4. Biofilm visualization with fluorescence microscopy

To visualize the effect of selected compounds on the bacterial biofilm formation, the biofilm was prepared with the same method as described earlier (2.6.1.) but in Petri plates (55 mm). The fluorescent probes, fluorescein diacetate (FDA), and propidium iodide (PI) (Sigma Aldrich, Steinheim, Germany), were applied to assess the viability of cells in the biofilm. Before the staining, a stock solution of FDA (1 mg/mL) in acetone and a stock solution of PI (1 mg/mL) in distilled water were prepared and stored in the refrigerator. After the biofilm was dried PBS buffer (1000 μL) containing 25 μL of FDA and 5 μL of PI were added to the samples. The plates were incubated with fluorescent dyes for 30 min at 30 °C in the dark. Next, the staining solution was removed, the biofilm was dried at the room temperature and examined under the fluorescence microscope Olympus BX53 (Olympus Corporation, Tokyo, Japan) equipped with specific wavelength filters set (FDA excitation/emission: 485/530; PI excitation/emission: 538/617). Biofilm of tested bacteria treated with sterile water were used as control samples.

#### 2.7.5. The mechanism of antimicrobial activity of QASs

The release of cell constituents was evaluated based on the modified method described by Paul et al.[28] and Zhang et al.[29] The cells of selected microorganisms (*S. aureus*, *P. aeruginosa* and *C. albicans*) from a fresh culture were centrifuged (at 8000 rpm, 5 min), suspended in 1 mL of sterile PBS with the addition of two compounds (**4** and **8**) in different concentrations (1000 μg/mL and 1*MIC) and incubated at 37 °C for 3 h. After incubation, the samples were centrifuged (at 8000 rpm, 5 min) and the supernatant was diluted in sterile water in the ratio 100 μL:900 μL. The efflux of cellular constituents was measured spectrophotometrically at a wavelength of 260 nm.

The fluorescent probe propidium iodide (PI) (Sigma Aldrich, Steinheim, Germany) was applied to assess the viability of selected microorganisms (*S. aureus* and *P. aeruginosa*). The stock solution of PI (1 mg/mL) was prepared in distilled water and stored in at 4 °C. Centrifuged cultures of bacteria treated with two selected compounds for 2 h were suspended in 5 mL of 50 mM phosphate buffer with the addition of 5 μL of PI at 30 °C for 15 min. Next, the staining solution was removed by centrifugation (8000 rpm, 1 min). The pellet was examined under the fluorescence microscope Olympus BX53 equipped with specific wavelength filter sets (CFDA excitation/emission: 485/530; PI excitation/emission: 538/617).

The cultures of *C. albicans* treated with two selected compounds for 2 h were centrifuged and transferred onto glass slides with and without methylene blue and photographed with a light microscope (Olympus BX53, Olympus Corporation, Tokyo, Japan) at 400× magnification. The cells treated with sterile water were used as control samples.

Changes in the morphology of selected bacteria: *S. aureus* and *P. aeruginosa* exposed to 0.5 and 1*MIC of compounds **4** and **8** for 24 h were assessed using a Zeiss EVO 10 scanning electron microscope with a STEM detector.

### 2.8. Solubility of the studied salts (**1**–**8**) and reference systems (**[NA][NIC]** and **[NA][PABA]**) in aqueous solutions of different pH

The solubilities of **1-8**, **[NA] [NIC]** and **[NA] [PABA]** were determined in SGF (pH = 1.2), distilled water (pH = 6.0) and PBS (pH = 7.4) by placing 1 g (±0.0001 g) of a tested compound in the round-bottom

flask and adding specific parts of aqueous solutions in portions until full dissolution. The samples were vigorously stirred for at least 5 min before the addition of the next portion of aqueous solutions, and the systems were thermostated at 36.6 °C (±0.1 °C). Finally, the analyzed compounds were divided into different solubility classes[30,31]. Three repetitions of the measurement were performed for each compound.

### 2.9. Stability of the studied salts (**4** and **8**) and reference systems (**[NA] [NIC]** and **[NA][PABA]**) in aqueous solutions of different pH

Stability of selected compounds: **4**, **8**, **[NA] [NIC]** , **[NA] [PABA]** , in different pH ((SGF (pH = 1.2), distilled water (pH = 6.0) and PBS (pH = 7.4)) were estimated for 50 μmol $L^{-1}$ aqueous solutions. Measurements were conducted in sealed glass vials containing a magnetic stir bar. All the vials had been shaken in a Heidolph MR Hei-End stirrer equipped with a Heat-On anodized block at a constant temperature of 36.6 °C (±0.1 °C) in the dark. After a period of time, a sample was collected from each vial and the absorbance of the solutions obtained was measured at $\lambda_{max}$ = 261-263 nm for the nicotinate anion, at $\lambda_{max}$ = 265-266 nm for the *p*-aminobenzoate anion, at $\lambda_{max}$ = 250-262 nm for **[NA] [NIC]** and at $\lambda_{max}$ = 251-268 nm for **[NA] [PABA]** using a VWR UV-6300PC spectrophotometer. The results are presented as the mean of three separate measurements.

### 2.10. Cytotoxicity to human intestinal cells

The cytotoxicity of the tested compounds (**1**-**8**, **[NA] [NIC]** or **[NA] [PABA]** ) and the reference pharmaceutical agent (benzalkonium chloride) was evaluated using the human normal small intestinal epithelial cell line, HIEC-6 (ATCC, CRL-3266), which was obtained from the American Type Culture Collection (ATCC, Manassas, VA, USA) and cultured according to the conditions recommended by ATCC. In the cytotoxicity experiments, the cells were grown in 96-well plates at an initial density of $2.5 \times 10^4$ cells/$cm^2$. After 24 h, the cells were treated with the analyzed compounds at concentrations of 1, 5, 10, 50 and 100 μg/mL for an additional 24 h under standard culture conditions. Before treatment, the compounds were dissolved in cell culture medium and sterilized by filtration through 0.22 μm pore membranes. The impact of the analyzed compounds on the human intestinal cells was assessed using an assay that measures the cleavage of the yellow dye MTT (3-(4,5-dimethylthiazol-2-yl)-2,5-diphenyltetrazolium bromide; Sigma–Aldrich). This cleavage produces purple formazan crystals, which are formed by mitochondrial dehydrogenase enzymes active only in living cells. After treatment, MTT solution was added to each well at a final concentration of 0.5 mg/mL, and the cell cultures were incubated at 37 °C for 3 h. Following incubation, the formazan crystals were extracted with acidic isopropanol for 20 min at room temperature. The absorbance was then measured at 570 and 690 nm using a Tecan M200 Infinite microplate reader (Tecan Group Ltd., Männedorf, Switzerland). Based on the results from the MTT assay, dose-response curves were plotted, and the cytotoxic doses ($IC_{10}$, $IC_{50}$, $IC_{90}$) of the tested compounds were determined.

### 2.11. Ecotoxicity towards aquatic life

To determine the $EC_{50}$ parameter for compounds, tests were carried out on marine crustaceans – *Artemia franciscana*. The methodology proposed in the Artoxkit M test (MicroBioTests Inc., Gent, Belgium), was developed according to the ASTM E1440-91 standard (American Society for Testing and Materials).

The hatching process was started first. For this purpose, 50 mg of cysts were transferred to the Petri dishes attached to the Artoxkit M set, which were then immersed in 10 mL of artificial sea water with salinity of 35‰ (a medium for the development of the tested organisms, as well as a solvent for preparing solutions of the tested compounds) and placed at a temperature of 25 °C, with access to light (6000–10,000 lux) for 30 h. Then, 2 h before placing them on the Artoxkit M plates, a 20 mg of spirulina was added to cultured artemia. In addition, 1 h before the analysis, the used sea water was oxygenated by passing a stream of air through the solution. To each of the 4 cells in a given row of a plate from the Artoxkit M kit, 1 mL of the solution at the specified concentrations (or the appropriate medium in the case of a control) were introduced. In the first column of cells (control sample and 5 selected concentrations) no less than 30 artemia specimens were placed from previously prepared Petri dishes. Then, from the first cell in the first column, artemia were collected at the selected concentration and added to the next three cells in the selected row, 10 organisms per cell. After introducing the organisms into the appropriate cells, the plates were covered with parafilm and then closed with a plastic cap. The prepared kit was incubated at 25 °C and protected from light. Number of motionless organisms were counted after 24 h and 48 h. Immobilization (Imm) was then calculated (eq. (2)) in relation to the number of organisms at the start of the test:

$$Imm = 100 \cdot \left(1 - \frac{No\ of\ mobile\ organisms}{No\ of\ mobile\ organisms\ at\ start}\right) \quad (2)$$

Next, the relationship between the effect and the concentration of the tested compounds was plotted, and based on this, the $EC_{50}$ was determined.

### 2.12. In silico bioavaliability predictions

The SMILES (Simplified Molecular Input Line Entry System) representations of ionic salts (**1**–**8**) and their non-ionic counterparts ( **[NA] [NIC]** and **[NA] [PABA]** ) were used for *in silico* bioavailability predictions, using the online SwissADME server.

### 2.13. Statistical analysis

To properly assess significant differences in the determined phytotoxic effects, a statistical analysis was performed using STATISTICA software. First, the one-way analysis of variance (ANOVA) test was performed to reveal if there were statistically significant differences between the tested groups (p value $< 0.05$). Tukey's posthoc test was used to calculate HSD (honestly significant difference) at the 5% level of significance. Different lowercase letters indicate significant differences between treatments.

## 3. Results and discussion

### 3.1. Synthesis and characterization of products

New active pharmaceutical ingredients (APIs) are essential for the development of innovative drug formulations with enhanced efficacy, stability, and bioavailability. APIs modifications in the form of salts, cocrystals or eutectics have garnered significant attention in pharmaceutical research, offering a powerful approach to improving the physicochemical properties, such as solubility, dissolution rate, and stability [5,32,33]. A promising strategy involves transforming APIs into ionic pairs, mostly known as quaternary ammonium salts (QASs), which, due to the presence of a long alkyl chain, contain a large, most often asymmetric organic cation. This type of structure not only influences compounds' lipophilicity but can also enhance membrane permeability, thereby improving biological activity[34–36]

In this work, two homologous series of QASs were synthesized using selected essential nutrients, i.e. various forms of vitamin B as starting materials. Initially, vitamin $B_3$ in the form of nicotinamide (NA) was subjected to quaternization, leading to the formation of *N*-alkylnicotinamide bromides with long alkyl chains ranging from hexyl to dodecyl. Next, through an ion exchange reaction, *N*-alkylnicotinamide ions were paired with another form of vitamin $B_3$, namely the anion of nicotinic acid (**1**–**4**) or with vitamin $B_{10}$, namely the anion of *p*-aminobenzoic acid

(**5**–**8**). As shown in Fig. 2, to investigate the potential benefits from the utilized API-QASs strategy, the ionic derivatives of vitamin B (**1**–**8**) were compared with reference substances deprived of ionic bonds and alkyl chains: a mixture of nicotinamide with nicotinic acid (**[NA] [NIC]**) and nicotinamide with *p*-aminobenzoic acid (**[NA] [PABA]**) as a cocrystal.

The synthesis of QASs **1**–**8**, based on the quaternization of NA and subsequent ion exchange of the bromide anion by nicotinate (**1**–**4**) or *p*-aminobenzoate (**5**–**8**), required different methods of purification of final products. It was noted that in contrast to nicotinates (**1**–**4**), *p*-aminobenzoates rapidly precipitated from cooled acetonic solution as yellow crystalline solids. In consequence, salts **1**–**4** were isolated *via* evaporation of acetone from filtrate after filtration, whereas the **5**–**8** precipitates were thoroughly separated and washed. As summarized in Table S2 (in Supporting Information), the yields of both steps were found to be high and exceed 80%; however, due to mentioned-above discrepancies in synthesis methodology, yields of *p*-aminobenzoates (**5**-**8**) were slightly lower. Obviously, the preparation of **[NA] [NIC]** and **[NA] [PABA]** did not require any purification step and these products were obtained with the highest yields (almost 100%). Structures of the synthesized salts **1**–**8** were confirmed by UV, FTIR, and $^{1}$H and $^{13}$C NMR spectroscopies. Their thorough analysis is provided in the Supporting Information (Figs. S1–S44).

The collected UV spectra indicated that reference co-crystal **[NA] [NIC]** exhibited two well-defined absorption maxima at 216 nm and 262 nm, with the former being approximately three times more intense, reflecting $\pi$–$\pi^*$ transitions localized mainly within the nicotinamide aromatic system. For its quaternized analogues (**1**–**4**) the overall spectral pattern remained similar; however, both bands underwent a noticeable hypsochromic shift, with the first maximum shifted to 200–205 nm and the second to 263 nm. This blue shift can be attributed to the electron withdrawal from the aromatic ring caused by the positively charged nitrogen atom in the quaternized system. For **[NA] [PABA]**, three distinct absorption maxima were observed at 204, 214, and 290 nm, all of comparable intensity (the molar absorption coefficients differing by less than 10%). In contrast, for PABA-based QASs (**5**–**8**) the two lower-wavelength bands merged into a single at 206–208 nm, which was accompanied by a second maximum at 273 nm. The latter represents a characteristic $\pi$–$\pi^*$ transition within the *p*-aminobenzoate aromatic system, which, compared to the non-ionic reference, was also shifted toward shorter wavelengths by approx. 17 nm. This bathochromic shift pattern suggests that PABA in **[NA] [PABA]** is present predominantly in its neutral (acidic) form, whereas in salts **5**–**8** it exists as the deprotonated anion.

FTIR analysis of spectra provided in the Supporting Information revealed that the C=O stretching vibration of the amide/COO group appeared at 1683 cm$^{-1}$ in the **[NA] [NIC]** and shifted slightly to approx. 1696 cm$^{-1}$ in the corresponding QASs (**1**–**4**), reflecting subtle electronic changes upon quaternization. Introduction of the alkyl chains led to a pronounced increase in the intensity of the aliphatic C–H stretching bands at 2850–3000 cm$^{-1}$, which was expected due to alkyl chain elongation. Additionally, the conversion from the acidic form (nicotinic acid) to the anionic form (nicotinate) resulted in an increase in intensity of the bands at 1550–1600 cm$^{-1}$, corresponding to COO asymmetric stretching vibrations, and a shift of the COO symmetric stretching vibrations from 1290 to 1430 cm$^{-1}$ in the **[NA] [NIC]** to 1370–1450 cm$^{-1}$ in salts **1**–**4**. A gradual increase in the intensity of aliphatic C–H stretching bands at 2800–3000 cm$^{-1}$ in the PABA-based QASs (**5**–**8**) is consistent with alkyl chain elongation. Moreover, the appearance of two distinct and intense bands at approximately 1530 cm$^{-1}$ and 1370 cm$^{-1}$, corresponding to the asymmetric and symmetric $COO^{-}$ stretching vibrations, respectively, confirms the presence of the PABA anion in these salts rather than its neutral acidic form, as also observed for **[NA] [PABA]**.

To highlight the electronic effects of quaternization, the $^{1}$H NMR spectrum of **[NA] [PABA]** was compared with that of the ionic compound **8** (Fig. S45). This comparison clearly illustrates the impact of alkyl chain introduction and the formation of the positively charged nitrogen on the chemical shifts in the aromatic region. Notably, the signals corresponding to the aromatic protons of nicotinamide in **[NA] [PABA]** (approx. 7.5–9.1 ppm) shifted toward higher values (deshielding) by up to 0.6 ppm in compound **8** (approx. 8.1–9.5 ppm), reflecting the substantial alteration of electron density caused by quaternization. The further comparison of the $^{1}$H NMR spectra revealed that among compounds **1**–**4** the signals from aromatic protons of nicotinate anion appeared at lower chemical shift values (7.5–9.1 ppm) compared to alkylated NA cations (approx. 8.3–9.6 ppm). Moreover, in all spectra signal from protons in amide ($CONH_2$) group is not visible, which is due to rapid proton–deuteron exchange with the deuterated solvent ($CD_3OD$). Generally, spectra of compounds **1**–**4** and **5**–**8** differed mainly in the relative intensities of the signals from the $CH_2$ groups of the alkyl chains (approx. 1.2–1.3 ppm). From the same alkyls, two triplets were observed at approximately 0.9 ppm (-$CH_2$-$CH_3$) and 4.5 ppm (N-$CH_2$-), as well as a multiplet signal around 2.0 ppm from the adjacent methylene group (N-$CH_2$-$CH_2$-). Analogous analysis of the $^{13}$C NMR spectra revealed that the signals corresponding to aromatic carbons appeared in the range of 125–172 ppm for products **1**–**4** and 115–176 ppm for products **5**–**8**, while the alkyl carbon signals were observed between 14 and 64 ppm in both series. The analysis of the chemical shift patterns, provided in the Supporting Information, is fully consistent with the expected structural features and confirms the successful formation of the desired QASs.

The molecular structures of compounds **1–8** were also confirmed by high-resolution LC/MS/TOF analysis (details regarding collected spectra are provided in the Supporting Information in Table S3). The observed *m/z* values for the quaternized nicotinamide cations were in excellent agreement with the calculated values: 207.1493 (calcd 207.1492) for **1**/**5**, 235.1805 (calcd 235.1805) for **2**/**6**, 263.2119 (calcd 263.2118) for **3**/**7**, and 291.2431 (calcd 291.2431) for **4**/**8**. The corresponding anions were also detected, with *m/z* values of 123.0555 for nicotinate (calcd 123.0320) and 138.0552 for PABA (calcd 138.0550). The consistency between the experimental and calculated values provides additional confirmation of the expected ionic structures.

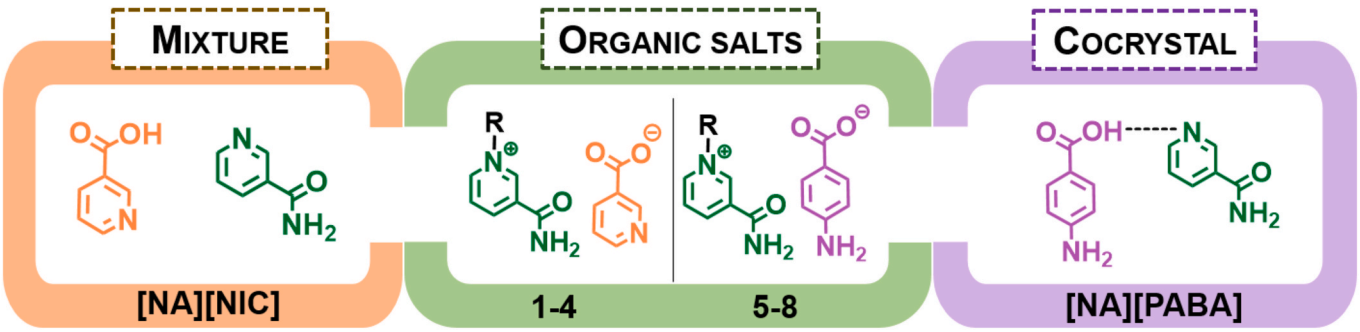


**Fig. 2.** Tested forms of APIs originated from nicotinamide and nicotinic or *p*-aminobenzoic acid.

Intriguingly, for all APIs in the form of QASs, it was not possible to determine a melting point (Table S2 in Supporting Information). It was noticed that **1**–**8** exhibited initial decomposition before melting, which was manifested by color shift from white or yellow to brown during heating. This may be due to the fact that in some ionic salts, particularly those with strong electrostatic interactions and high lattice structure, the energy required to overcome these forces is too high for classical melting to occur. Instead, upon reaching a temperature of melting, the phenomenon of decomposition of certain functional groups occurs faster. As a result, there is no distinct melting point, similar to most ionic liquids, because the process involves chemical decomposition rather than a phase transition [34,37]. Theoretically, **1**–**8** should exhibit thermal stability at least similar to their analogues, and notable degradation was expected to appear above 150 °C [22]. To examine this phenomenon in greater detail, we measured the melting points of the potassium salts of NIC and PABA, the precursor components for the synthesis of compounds **1**–**8**. The melting point of [K][PABA] was found to be 206–208 °C, whereas for [K][NIC], no melting was observed even at 300 °C, indicating its high thermal stability. Therefore, the lower stability of the synthesized ion pairs may be due to the specific cation-anion interactions in the combination of alkylated NA with NIC or PABA, leading to alterations in electron density in the aromatic ring of the cation, which is relatively the most susceptible to decomposition.

Interestingly, **[NA] [NIC]** and **[NA] [PABA]** behaved differently in comparison to the obtained QASs. As a result of mixing nicotinic acid and nicotinamide, instead of a sharp melting point, the formed mixture exhibited a broader melting range; however, the melting starts at a lower temperature than that of the starting components (121–188 °C). This suggests occurrence of a physical mixture with limited ability to form an eutectic, in which carboxylic acid and amide form strong dimers through hydrogen bonding [38]. Assuming that these dimers are more stable than potential new intermolecular interactions, one can conclude that the mixture does not form a homogeneous eutectic phase but rather a system in which separate dimers of both compounds coexist. In this case, only partial interactions between the components that may occur, are not strong enough to generate homogeneous phase [39]. Consequently, the mixture does not exhibit a sharp melting point but instead undergoes gradual melting due to the coexistence of two crystalline phases. A similar phenomenon was observed with a mixture of isonicotinamide and benzoic acid, where a double melting point with a wide temperature range (depending on the amide content) was noted [40]. Interestingly, in the case of a mixture of NA with PABA, a clearly defined melting point (109–111 °C) was determined. Based on the similar results obtained for the cocrystal of nicotinamide and salicylic acid [21,41], the formation of a cocrystal can also be inferred, indicating a stable arrangement between the two components - NA and PABA.

The analysis of water content showed that in both homologous series, regardless of the anion, the percentage decreased as the alkyl chain length increased. This demonstrates the clear influence of the chain length on the parameter while attributing hydrophobic properties to the compounds. For **1**–**4**, the water content values ranged from 1.30% to 1.88%, while for **5**–**8** the collected results varied from 0.94% to 2.16%. The lowest water contents were reported for **[NA] [NIC]** and **[NA] [PABA]**, 0.63 and 0.56% accordingly, which may suggest that the absence of an alkyl chain or specific ionic interactions within their structures influence the affinity to water molecules. In addition, compounds analyzed in this study were assessed as non-hygroscopic in long-term contact with air (60% humidity) at room temperature, which may be seen as an additional advantage for drug preservation. The non-ionic compositions **[NA] [NIC]** and **[NA] [PABA]** were exceptions, as after 5 days of exposure to air their water content increased by 3-fold and 2-fold, respectively (values are provided in the Supporting Information, Table S2). This set of results underscores the beneficial impact of the API's form, which not only affects the formulation efficacy but also plays a crucial role in proper storage conditions.

The purity of the dried products (**1**–**8**) was evaluated using three independent analytical methods: two-phase titration in accordance with EN ISO 2871-1:2010, LC/MS/TOF analysis, and elemental analysis (CHN). The results listed in Table S3 (Supporting Information) showed very good consistency between the methods, confirming the high purity of the synthesized compounds. For most products the values exceeded 98.5%. Minor deviations (±0.4%) between the theoretical and experimental CHN values can be attributed to the presence of water (approximately 0.5–2%), which slightly increased the hydrogen content in the elemental composition. Both the two-phase titration and LC/MS/TOF analyses confirmed the high purity of the products, with clear and reproducible phase color changes observed for compounds containing alkyl chains of at least $C_8H_{17}$ (**2**–**4** and **6**–**8**). For **1** and **5**, which possess shorter alkyl chain ($C_6H_{13}$), reliable titration results could not be obtained; however, their purity was verified by LC/MS/TOF (99.2% and 98.5%, respectively).

### 3.2. Octanol–water partition coefficient

The octanol-water partition coefficient (log $K_{OW}$) is a key parameter in drug design, particularly for orally administered drugs. Excessively high log $K_{OW}$ (higher than 5) indicates excessive lipophilicity, reducing water solubility and limiting bioavailability. Conversely, a very low log $K_{OW}$ (below 0) reflects to high hydrophilicity, hindering membrane permeation. Hence, an optimal log $K_{OW}$, in a region between 0 and 3, ensures a good balance between water solubility, facilitating absorption in the gastrointestinal tract, enabling effective membrane permeability [42].

As shown in Fig. 3A, the log $K_{OW}$ values measured for the tested compounds occurred in a range from approx. −1.73 to 0.35 (exact values are provided in Table S4, Supporting Information). The gathered data clearly indicate that APIs derived from nicotinate (**1**–**4**) exhibit higher lipophilicity compared to salts with PABA (**5**–**8**). In effect values noted for **3** and **4** are close to the optimal log $K_{OW}$ range. In the case of APIs containing a component derived from PABA, only **8** exhibits optimal properties for use as an oral drug. Interestingly, the non-alkylated compounds, **[NA] [NIC]** and **[NA] [PABA]** turned out to be less hydrophilic than their ionic analogues containing shorter alkyl substituent: hexyl (**1** and **5**) or octyl (**2** and **6**), accordingly. This observation suggests that not only the length of alkyl chain, but also the structural elements originating from the specific components, like occurrence of ionic interactions, can significantly influence compounds' lipophilic character.

Comparison of the synthesized **1**–**8** with their parent *N*-alkylnicotinamide bromides (**P1**–**P4**), as shown in Table S4 (in Supporting Information), revealed that anion exchange generally resulted in lower log $K_{OW}$ values ($\Delta\log K_{OW} = -1.28$ to $-0.18$), indicating an increase in hydrophilic character after ion exchange. This outcome was somewhat unexpected, as in many QAS systems anion replacement (*e.g.*, chloride to organic anion) often increases lipophilicity. Nevertheless, the resulting log $K_{OW}$ values for compounds **3**, **4**, and **8** are close to or within the optimal range (0–3) for oral drug candidates, suggesting that the modified salts maintain a favorable balance between membrane permeability and aqueous solubility (increased hydrophilicity after anion exchange reduces the risk of API precipitation in aqueous systems). Importantly, the ion-exchange process also provides additional formulation benefits: the bromide salts tended to form viscous or gel-like systems even at low concentrations, which may significantly hinder reproducible dosing and oral delivery. Moreover, replacing the inert bromide anion with biologically active counterions, such as nicotinate or *p*-aminobenzoate introduces pharmacologically beneficial moieties, potentially enhancing overall biocompatibility and therapeutic value.

Overall, the lipophilicity of the studied compounds is primarily governed by the alkyl chain length, with longer chains increasing log $K_{OW}$ values, while the nature of the counterion further modulates this parameter. In particular, nicotinate-based salts (**1**–**4**) exhibit higher lipophilicity than their *p*-aminobenzoate analogues (**5**–**8**), highlighting

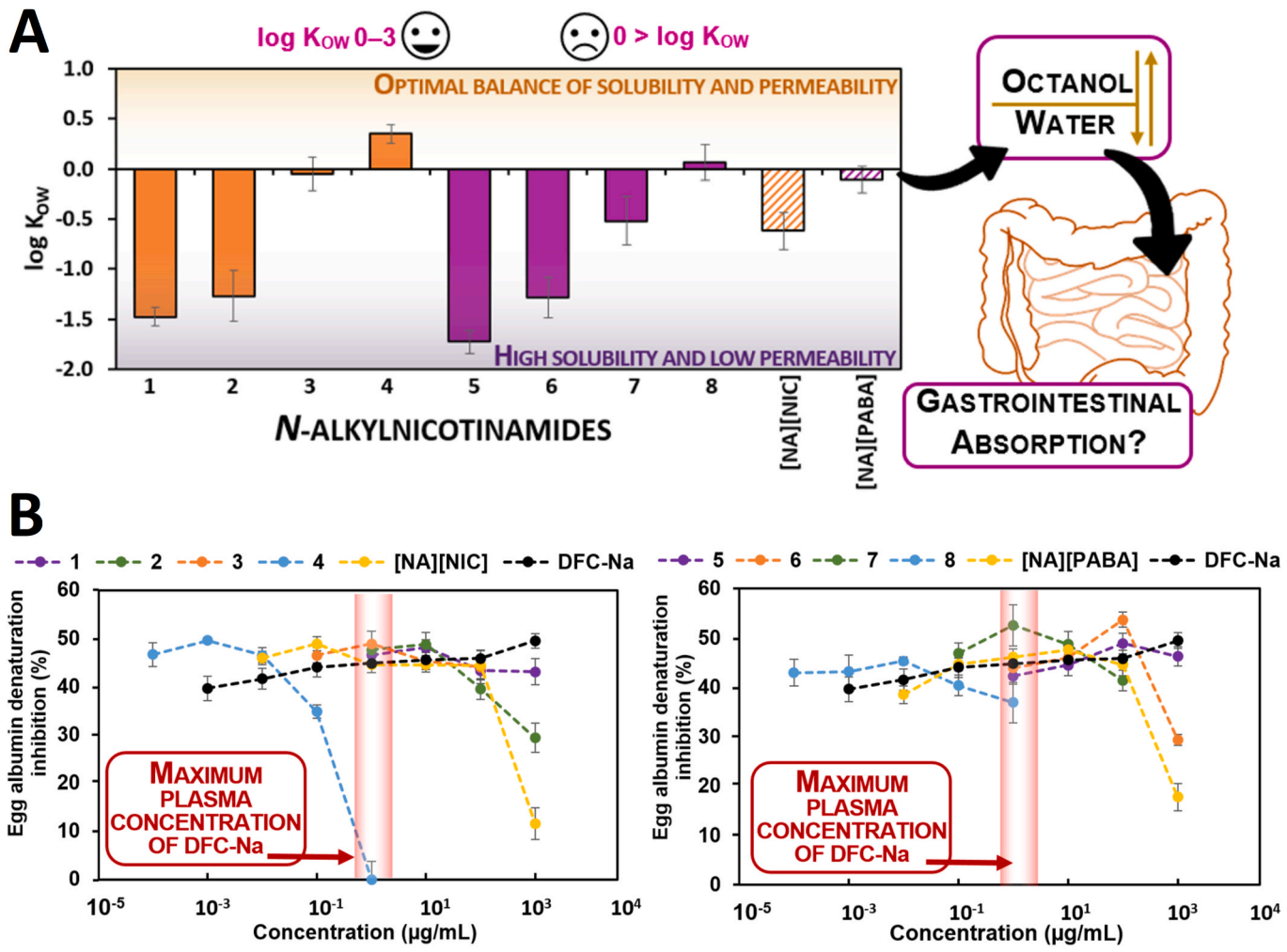


**Fig. 3.** Octanol–water partition coefficient values for *N*-alkylnicotinamide nicotinates (**1-4**), *N*-alkylnicotinamide *p*-aminobenzoates (**5-8**), **[NA] [NIC]** and **[NA] [PABA]** (**A**); egg albumin denaturation inhibition for *N*-alkylnicotinamide nicotinates (**1-4**), *N*-alkylnicotinamide *p*-aminobenzoates (**5-8**), **[NA] [NIC]**, **[NA] [PABA]** and diclofenac sodium (DFC-Na) (**B**).

the combined influence of both structural elements.

Notably, many pharmaceuticals administered *via* oral route exhibit good hydrophilic properties, which is manifested by their low log $K_{OW}$ values. In contrast, some anti-inflammatory drugs, even in their ionic form with sodium as the counterion, exhibit a relatively high log $K_{OW}$, indicating their higher lipophilic character. Noteworthy examples from these two groups include metformin, thiamine, ciprofloxacin, ibuprofen sodium and diclofenac sodium with their log $K_{OW}$ values as follows: −1.43, −2.04, −1.09, 0.92 and 0.69 respectively [43–47]. Undeniably, log $K_{OW}$ is a valuable parameter that facilitates to evaluate permeability and bioavailability of various biologically active substances. However, it may not fully capture the complexity of pharmacokinetics of specific group of compounds, especially when considering drug permeability in a complex environment such as the human body. Therefore, a comprehensive assessment integrating additional parameters, such as solubility, protein binding, or active transport mechanisms, is essential for a more accurate evaluation of novel APIs' pharmacokinetic properties and therapeutic potential.

### 3.3. *Anti-inflammatory potential: egg albumin denaturation assay and molecular docking studies*

During infections, inflammatory responses are often triggered as a natural defense mechanism to combat pathogens. Anti-inflammatory and antiseptic agents, when used simultaneously, may exhibit complementary effects by reducing inflammation. This synergistic interaction can enhance therapeutic outcomes and promote more efficient recovery from infections [48,49]. As reported in the literature, NA exhibits anti-inflammatory properties, although it is not classified as a conventional anti-inflammatory drug. Its effects are primarily attributed to its influence on cellular metabolic pathways, as well as the regulation of oxidative stress and immune responses [50]. Studying the potential anti-inflammatory activity of ionic derivatives of NA, such as salts **1**–**8**, can provide valuable outcomes, as these combinations may lead to synergistic effects and result in a new approach to treating inflammatory conditions. Hypothetically, long alkyl chain improves membrane penetration, while the anions can additionally modify interactions with receptors and inflammatory pathways. In this context, an appropriate analysis using the egg albumin assay was performed for both ionic (**1**–**8**) and non-ionic products (**[NA] [NIC]** and **[NA] [PABA]**). The results of egg albumin denaturation assay are shown in Fig. 3B (values can be found in Table S5, Supporting Information).

The collected results revealed that the highest activity in the egg albumin denaturation were observed for compounds comprising octyl (**6**) or decyl (**7**) chains in the NA cation and PABA anion, with values equal to 53.7% and 52.6%, respectively. Moreover, the vast majority of the analyzed compounds exhibited greater activity than the commonly used drug - diclofenac sodium salt (DFC-Na) at its maximum plasma concentration in the human body (1.4–3.0 μg/mL) [51], marked with red color in Fig. 3B. In this specific region, all nicotinates (**1**–**4**) were

found to be more effective at inhibiting albumin denaturation in comparison to DFC-Na, whereas among QASs with PABA anion the enhancement was noted only for salt **7**. In comparison, the reference compound (DFC-Na) achieved a similar level of activity (49.5%) only at concentration of 1000 μg/mL. Compounds deprived of alkyl chain in their structure, **[NA] [NIC]** and **[NA] [PABA]**, were also effective in inhibiting protein denaturation in a broad range of concentrations. Remarkably, the QAS strategy allowed for a significant reduction of the therapeutic dose by even several orders of magnitude. The nicotinate comprising the longest chain (**4**) exhibited a remarkable activity of 49.6% at a concentration as low as 0.001 μg/mL. Furthermore, the ability to prevent egg albumin denaturation of **1**–**8** increases with the alkyl chain elongation; it reaches increasingly higher values at lower concentrations, while at higher concentrations all compounds appear to promote denaturation. This observation clearly indicates that only a specific chain length can cause a significant shift in the zone in which the substance exerts a beneficial effect on the prevention of egg albumin denaturation. In consequence, among tested salts **1**–**8**, only in the case of those containing the longest dodecyl substituent (**4** and **8**) exhibited a pronounced shift of beneficial egg albumin denaturation inhibition towards significantly lower API concentrations. These results indicate also that the alkyl chain length is the predominant structural determinant of the anti-inflammatory response within the investigated series. Increasing the hydrophobic chain from hexyl to decyl/dodecyl shifted the effective concentration range towards markedly lower concentrations, whereas the effect of the anion was comparatively smaller. Nevertheless, the counterion was not biologically irrelevant: nicotinate- and PABA-containing analogues with the same cationic chain length often differed in their degree of albumin protection, indicating that the aromatic head group and its functional groups can additionally modulate the activity. Thus, the observed anti-inflammatory effect appears to result from a balance between hydrophobic interactions provided by the alkyl chain and specific interactions associated with the ionic head groups. Nonetheless, it should be emphasized that all studied compounds exhibit greater potential anti-inflammatory activity than DFC-Na at certain concentrations, which supports further research to evaluate their potential as an attractive alternative for combating inflammation.

NA has been studied for its anti-inflammatory effects in the treatment of acne vulgaris when administered orally. The results of this research show significant improvement with combination therapies containing nicotinamide, azelaic acid, zinc, pyridoxine, copper, and folic acid [52]. Notably, the anti-inflammatory properties of alkylated nicotinamide forms have already been demonstrated and analyzed in our previous work. Molecular docking studies confirmed these properties, with the compound containing a long alkyl chain (dodecyl) exhibiting the highest anti-inflammatory activity, consistent with *in vitro* results on egg albumin [21]. Nicotinic acid has been found to significantly reduce inflammation in vascular lesions in mice, leading to a 30% decrease in total lesion area compared to the control group, highlighting its potential as a therapeutic agent for vascular diseases [53]. Furthermore, studies have confirmed the anti-inflammatory effects of nicotinic acid in human monocytes, showing a reduction in the secretion of proinflammatory mediators by up to 60% [54]. Additionally, PABA enclosed in a cocrystal with ketoprofen demonstrated superior anti-inflammatory efficacy compared to ketoprofen alone. *In vitro* studies using the egg albumin method showed a response nearly twice as strong as that of the pure drug [55]. The different methods of obtaining the mentioned results make it impossible to draw firm conclusions. However, the findings for the PABA cocrystal suggest that even a simple structural modification of one form of vitamin B can significantly enhance its efficacy and unlock its therapeutic potential in terms of anti-inflammatory properties.

Molecular docking simulations were employed to evaluate the potential interactions between the studied compounds and the cyclooxygenase-2 (COX-2) enzyme. This approach provides an effective *in silico* tool for predicting ligand–protein complementarity and binding strength, correlating well with experimental inhibition data in nonsteroidal anti-inflammatory drugs (NSAIDs) [56]. All ligands were found to be docked within the same primary binding cavity (Pocket C1) encompassing the key catalytic residues: **R120**, **Y385**, and **S530**; and the stabilizing residues: **L352**, **S353**, and **V523**, which collectively define the COX-2 active channel. The resulting Vina scores ranged from −8.0 to −5.3 kcal $mol^{-1}$, confirming a consistent binding mode across the tested series (all data are listed in Table S6 in Supporting information). As expected, DFC-Na exhibited strong affinity (−7.0 kcal $mol^{-1}$) through interactions with **Y385** and **S530**, both directly involved in arachidonic acid oxidation. Remarkably, the QASs cations demonstrated a clear chain-length-dependent enhancement in binding affinity. Starting from −7.0 kcal $mol^{-1}$ for the shortest alkyls (**1** and **4**) the affinity was improving progressively to −7.5 kcal $mol^{-1}$ for the longest chain derivative among nicotinate series (**4**), and even further to −8.0 kcal $mol^{-1}$ for **8** in the PABA series. The strongest binders comprising $C_{10}$ and $C_{12}$ alkyls formed simultaneous interactions with all six key residues: **R120**, **Y385**, **S530**, **L352**, **S353**, and **V523**, indicating a near-complete engagement of the COX-2 binding pocket. The extended alkyl chains likely enhance hydrophobic complementarity within the lipophilic channel, strengthening van der Waals and π–alkyl interactions with **V523** and **L352**, while the positively charged ammonium head enables electrostatic stabilization near **R120**. In contrast, the anionic counterparts (nicotinate and PABA) exhibited weaker binding (−5.3 to −5.9 kcal $mol^{-1}$), involving only the stabilizing residues and lacking direct interactions with the catalytic triad. This supports their auxiliary role in molecular recognition, contributing to solubility and ionic pairing rather than enzymatic inhibition. Similarly, the nonionic systems comprising nicotinamide, nicotinic acid, and PABA acid, displayed modest affinities (−5.3 to −6.0 kcal $mol^{-1}$) caused by the absence of a positively charged center and reduced hydrophobicity. These findings reveal a distinct structure–activity relationship (SAR): increasing the alkyl chain length in QASs directly enhances COX-2 binding affinity, surpassing that of diclofenac. The data suggest that long chain QASs, comprising $C_{10}$–$C_{12}$ alkyls in cations, may act as novel anti-inflammatory compounds, capable of mimicking or exceeding the binding efficiency of conventional NSAIDs.

Taken together, the docking results provide a molecular rationale for the experimentally observed chain-length dependence of the anti-inflammatory activity. The alkyl chain appears to be the major structural element controlling access to and hydrophobic complementarity within the COX-2 channel, whereas the nicotinate or PABA anion contributes mainly through ionic pairing and modulation of molecular recognition. This distinction is consistent with the experimental data, in which changes in alkyl chain length produced a substantially stronger effect on activity than exchange of the counterion. The positively charged quaternary nitrogen therefore appears to provide an important anchoring element, while the hydrophobic chain determines the extent of interaction with the lipophilic region of the binding site.

### 3.4. Antimicrobial activity

#### 3.4.1. MIC and MBC/MFC determination

In an era of increasing resistance of microorganisms to antibiotics, the search for new, effective bactericides is becoming an integral part of modern pharmacy. In this context, the salts obtained in the present work were examined towards broad spectrum of microorganisms including Gram-positive and Gram-negative bacteria, yeasts and filamentous fungi. As the results in Table 1 show, the antibacterial and antifungal properties of tested compounds varied depending on the compound and microorganism.

The antimicrobial activity of the tested salts **1**–**8** increases with the alkyl chain elongation. Salts **4** and **8** containing the longest dodecyl substituent demonstrated the highest antimicrobial activity with MIC values ranging from 7.81 to 125 μg/mL against Gram-negative bacteria, 3.9 to 31.25 μg/mL against Gram-positive bacteria and 3.9 (**8**) or 7.81

**Table 1**
Antimicrobial activity of *N*-alkylnicotinamide nicotinates (**1**-**4**), *N*-alkylnicotinamide *p*-aminobenzoates (**5**-**8**), **[NA] [NIC]**, **[NA] [PABA]**, calculated as MIC and MBC/MFC.

| Microorganism | MIC/MBC/MFC [μg/mL] | Tested compounds | | | | | | | | | |
|---|---|---|---|---|---|---|---|---|---|---|---|
| | | 1 | 2 | 3 | 4 | 5 | 6 | 7 | 8 | [NA] [NIC] | [NA] [PABA] |
| **Gram-negative bacteria** | | | | | | | | | | | |
| ***P. aeruginosa* ATCC 9027** | MIC | >1000 | >1000 | 500 | 125 | >1000 | 1000 | 500 | 125 | >1000 | >1000 |
| | MBC | >1000 | >1000 | 500 | 125 | >1000 | >1000 | 500 | 125 | >1000 | >1000 |
| ***E. coli* ATCC 25922** | MIC | >1000 | 1000 | 250 | 31.5 | >1000 | 1000 | 250 | 62.5 | >1000 | >1000 |
| | MBC | >1000 | 1000 | 250 | 31.5 | >1000 | 1000 | 500 | 62.5 | >1000 | >1000 |
| ***M. catarrhalis* ATCC 25238** | MIC | >1000 | 1000 | 125 | 7.81 | >1000 | 1000 | 250 | 7.81 | >1000 | >1000 |
| | MBC | >1000 | 1000 | 125 | 15.63 | >1000 | 1000 | 500 | 15.63 | >1000 | >1000 |
| ***S. marcescens* ATCC 8100** | MIC | >1000 | 1000 | 250 | 15.63 | >1000 | >1000 | 250 | 15.63 | >1000 | 1000 |
| | MBC | >1000 | >1000 | 250 | 31.25 | >1000 | >1000 | 250 | 15.63 | >1000 | >1000 |
| ***C. jejuni* ATCC 33291** | MIC | >1000 | >1000 | 250 | 15.63 | >1000 | >1000 | 250 | 15.63 | >1000 | >1000 |
| | MBC | >1000 | >1000 | 250 | 31.25 | >1000 | >1000 | 500 | 15.63 | >1000 | >1000 |
| ***S. Enteritidis* ATCC 13076** | MIC | >1000 | >1000 | 250 | 15.63 | >1000 | >1000 | 250 | 15.63 | 500 | >1000 |
| | MBC | >1000 | >1000 | 250 | 31.25 | >1000 | >1000 | 500 | 31.25 | 1000 | >1000 |
| ***P. vulgaris* ATCC 49132** | MIC | >1000 | >1000 | 1000 | 125 | >1000 | >1000 | 1000 | 125 | >1000 | >1000 |
| | MBC | >1000 | >1000 | 1000 | 125 | >1000 | >1000 | 1000 | 125 | >1000 | >1000 |
| **Gram-positive bacteria** | | | | | | | | | | | |
| ***L.monocytogenes* ATCC 19111** | MIC | >1000 | 1000 | 250 | 31.25 | >1000 | >1000 | 250 | 31.25 | >1000 | >1000 |
| | MBC | >1000 | >1000 | >1000 | 31.25 | >1000 | >1000 | >1000 | 31.25 | >1000 | >1000 |
| ***M. luteus* ATCC 4698** | MIC | >1000 | >1000 | 250 | 31.25 | >1000 | >1000 | 250 | 15.63 | >1000 | 1000 |
| | MBC | >1000 | >1000 | 1000 | 62.5 | >1000 | >1000 | 500 | 31.25 | >1000 | 1000 |
| ***E. faecalis* ATCC 19433** | MIC | >1000 | >1000 | 250 | 15.63 | >1000 | 1000 | 250 | 15.63 | >1000 | >1000 |
| | MBC | >1000 | >1000 | 250 | 62.5 | >1000 | >1000 | 500 | 31.25 | >1000 | >1000 |
| ***S. aureus* ATCC 33862** | MIC | >1000 | 500 | 62.5 | 3.9 | >1000 | 500 | 62.5 | 3.9 | 1000 | 1000 |
| | MBC | >1000 | 500 | 62.5 | 7.81 | >1000 | 500 | 62.5 | 3.9 | >1000 | >1000 |
| ***B. subtilis* DSM 4451** | MIC | >1000 | >1000 | 250 | 3.9 | >1000 | >1000 | 125 | 15.63 | >1000 | 1000 |
| | MBC | >1000 | >1000 | 1000 | 7.81 | >1000 | >1000 | 125 | 15.63 | >1000 | 1000 |
| **Fungi** | | | | | | | | | | | |
| ***C. albicans* ATCC 10231** | MIC | >1000 | >1000 | 500 | 62.5 | >1000 | >1000 | 1000 | 62.5 | >1000 | >1000 |
| | MFC | >1000 | >1000 | 500 | 62.5 | >1000 | >1000 | 1000 | 125 | >1000 | >1000 |
| ***R. mucilaginosa* PUEB** | MIC | >1000 | >1000 | 250 | 62.5 | >1000 | 1000 | 500 | 62.5 | >1000 | >1000 |
| | MFC | >1000 | >1000 | 250 | 62.5 | >1000 | 1000 | 500 | 62.5 | >1000 | >1000 |
| ***C. neoformans* ATCC 14116** | MIC | >1000 | 250 | 31.25 | 7.81 | 1000 | 250 | 62.5 | 3.9 | >1000 | 1000 |
| | MFC | >1000 | 500 | 62.5 | 7.81 | 1000 | 500 | 62.5 | 3.9 | >1000 | 1000 |

(**4**) to 62.5 μg/mL against fungi. Salts **3** and **7** showed much lower effectiveness in the microbial growth inhibition with MIC values from 125 to 1000 μg/mL against Gam-negative bacteria, 62 to 250 μg/mL against Gram-positive bacteria, while antifungal properties ranged from 31.25 to 500 μg/mL in case of salt **3** and 62.5 to 1000 μg/mL for salt **7**. Salts **2** and **4** exhibited activity only towards selected microorganisms in the concentration 250 – 1000 μg/mL, while compounds **1** and **5** with the shortest substituent did not show antimicrobial activity in the concentration range studied. The tested compounds showed a stronger effect on Gram-positive bacteria compared to Gram-negative bacteria and fungi, which is often observed in the case of QASs. This is due to the different structure of the cell wall, which in Gram-positive bacteria is composed of many layers of peptidoglycan, while Gram-negative strains have a thinner peptidoglycan layer and an outer membrane composed of proteins and lipopolysaccharides (LPS), which makes it difficult for antibacterial agents to penetrate [57]. It should be acknowledged that *N*-alkylnicotinamide derivatives with salicylate anion showed generally lower bactericidal efficacy against *S. aureus*, *C. albicans* and *P. aeruginosa* compared to salts with nicotinate and *p*-aminobenzoate anion, with even 2-fold differences in MIC values. This clearly demonstrates that not only the length of the alkyl chain, but also the individual components of the compound as well as the specific interactions between them, affect their biological activity [21].

To highlight the electronic effects of quaternization the effect of alkyl chain length and anion type on biological activity, the sum of MIC or MBC/MFC values, and concentrations corresponding to maximum inhibition of albumin denaturation were compared in Figs. S46 and S47 (in Supporting Information). The Structure–Activity Relationship (SAR) analysis revealed that the alkyl chain length has a crucial impact on both antimicrobial and protein-stabilizing properties. Consequently, QASs with a $C_6$ chain (**1** and **5**) exhibited the lowest activity in both assays, whereas extending the chain to $C_8$ (**2** and **6**) resulted in a pronounced improvement in antimicrobial efficacy. Interestingly, the nonionic references (**[NA] [NIC]** and **[NA] [PABA]**), despite their negligible antimicrobial activity, showed relatively strong protein-stabilizing effects. This suggests that nonionic interactions between API molecules can promote protein structure stabilization, while the presence of a long alkyl chain, in agreement with literature reports, enhances affinity for microbial membranes and thereby improves antimicrobial potency [58, 59]. Further chain elongation to $C_{10}$ (**3** and **7**) and $C_{12}$ (**4** and **8**) led to a synergistic enhancement of both biological functions. The longer alkyl substituents not only strengthened antimicrobial activity but also reduced the concentration required for maximum inhibition of protein denaturation, indicating higher efficiency at lower doses (an important aspect from a pharmacological safety perspective). Interestingly, the nicotinate salt (**4**) exhibited superior overall biological performance

compared to its *p*-aminobenzoate analogue (**8**), suggesting that the presence of the pyridine ring may facilitate additional electrostatic or π–π interactions with biomolecules, contributing to enhanced bioactivity. In summary, extension of the alkyl chain promotes a synergistic improvement in both antimicrobial and protein stabilization properties, while the nature of the counterion fine-tunes the molecular interactions and overall bioefficacy.

The results of antimicrobial activity by well-diffusion assay, presented in Table S7 and Fig. S48 in Supporting Information, demonstrate that the efficacy of the tested compounds depended on both the chemical structure of the compound and the indicator microorganism. Among the investigated derivatives, compounds **4** and **8** exhibited the highest antimicrobial activity, producing the largest growth inhibition zones. Interestingly, no inhibition zones were observed for several compound–microorganism combinations despite previously determined MIC and MBC values of 500 μg/mL. This phenomenon may be related to the different principles underlying the two methods. In the agar diffusion assay, antimicrobial activity depends not only on the intrinsic

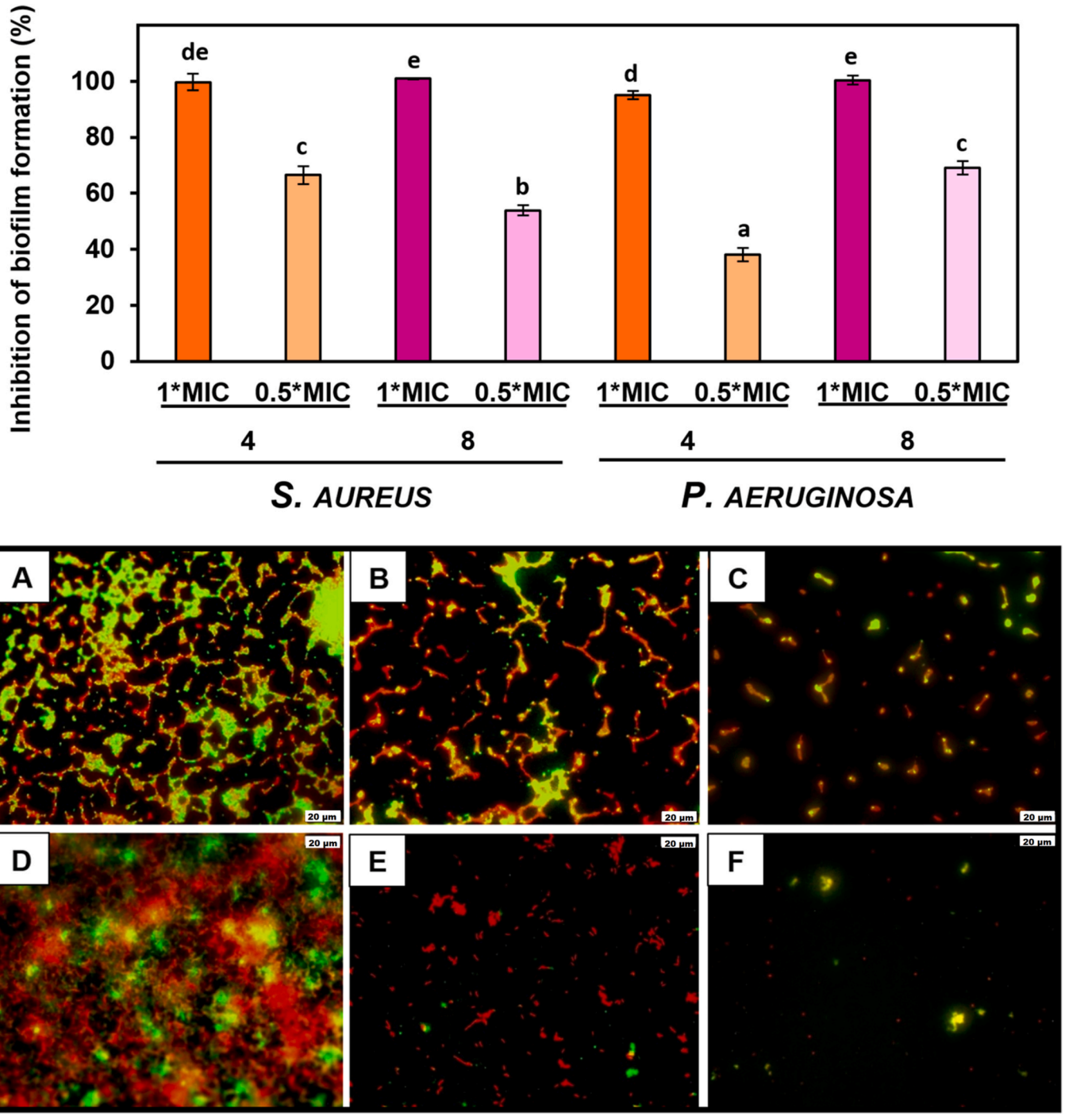


**Fig. 4.** Inhibition of biofilm formation by *S. aureus* and *P. aeruginosa*: for compound **4** – 1*MIC = 3.9 μg/ml, 0.5*MIC = 1.95 μg/ml; for compound **8** - 1*MIC = 125.0 μg/ml, 0.5*MIC = 62.5 μg/ml. Averages with different letters (a–e) are significantly different at the $p < 0.05$ (upper graph); effects of **4** and **8** on *S. aureus* and *P. aeruginosa* biofilm formation at a concentration 1*MIC: (A) Untreated biofilm formed by *S. aureus* – control; (B) Biofilm formed by *S. aureus* treated with **4**; (C) Biofilm formed by *S. aureus* treated with **8**; (D) Untreated biofilm formed by *P. aeruginosa* – control; (E) Biofilm formed by *P. aeruginosa* treated with **4**; (F) Biofilm formed *by P. aeruginosa* treated with **8**.

activity of the compound but also on its ability to diffuse through the solid medium. In contrast, the microdilution assay measures the direct interaction of the compound with microbial cells in a liquid environment. Therefore, compounds exhibiting limited diffusion in agar may produce weak or undetectable inhibition zones despite measurable antimicrobial activity determined by MIC and MBC assays.

### 3.4.2. Antibiofilm properties

It is estimated that up to 80% of microbial infections are associated with the presence of a biofilm. Its formation therefore plays a key role in the course of many infections, including in the oral cavity, gastrointestinal or urinary tract and wounds [60]. Biofilm is a complex bacterial community that, due to its multidimensional structure, provides protection against antimicrobial agents, promotes the development of drug resistance, and may even protect the microorganisms from the host's immune system [61]. Conventional approaches to treating biofilm infections are often insufficient and often require an increase in the dose and duration of antibiotic use, which in turn may lead to the development of drug resistance [62]. Therefore, the antibiofilm properties of the prepared compounds were determined.

Salts with the highest antimicrobial activity (**4** and **8**) were chosen and their effect on the biofilm formation by *S. aureus* and *P. aeruginosa* at a concentration corresponding to 0.5 and 1*MIC were investigated (Fig. 4). At lower concentration, the analyzed compounds did not show full efficacy against biofilm. Inhibition values for its formation ranged from approx. 40 to 70%. Fascinatingly, the results show that both of them at a concentration of 1*MIC fully inhibited biofilm formation by *S. aureus*, while in the case of *P. aeruginosa* the effectiveness is dependent on the compound. While **8** completely inhibited biofilm formation, **4** exhibited a slightly reduced effectiveness of 95%.

Fluorescence microscopy was used to visualize the effect of selected salts on the degree of biofilm formation by *S. aureus* and *P. aeruginosa* bacteria at a concentration of 1*MIC (Fig. 4). Intense staining in the control samples indicates almost complete coverage of the tested surface with biofilm, with a dominant share of live cells (green fluorescence), whereas in the samples treated with selected salts, only small clusters of cells with a dominant share of dead cells (red fluorescence) appear on the surface. Studies on the effectiveness of biofilm growth inhibition confirm the high antimicrobial activity of the analyzed compounds not only limited to direct action against specific bacterial strains, but also contributes to hindering of their potential defense mechanisms [63].

### 3.4.3. The mechanism of antimicrobial activity of QASs

To elucidate the effects of **4** and **8** on microbial cells, *S. aureus, P. aeruginosa*, and *C. albicans* were selected as representative organisms. The cells were treated with the test compounds at concentrations corresponding to the MIC and 1000 mM, and the release of cellular components was evaluated after 2 h of incubation *via* spectrophotometric analysis (Table 2). In all cases, treatment with **4** and **8** led to an increase in $OD_{260\ nm}$ values, indicating the leakage of intracellular material. Such release of cytoplasmic components is indicative of severe and irreversible damage to the cytoplasmic and plasma membranes [64].

Fluorescence microscopy data, presented in Fig. 5, further confirmed bacterial cell envelope damage. The bacterial cell membrane integrity was assessed by staining with propidium iodide (PI), a DNA-binding dye that emits fluorescence only after entering cells with membrane damage. Generally, viable cells with intact membranes remain nonfluorescent, whereas nonviable cells with membrane damage exhibit a red fluorescence signal. As shown in Fig. 5, control cells showed only minimal red fluorescence, indicating preserved membrane integrity. In contrast, cells treated with **4** and **8** showed a marked, concentration-dependent increase in red fluorescence, consistent with significant membrane damage. Propidium iodide is widely used as an indicator of membrane permeability and constitutes one of the key probes employed in live/dead viability assays. Therefore, the observed increase in PI-positive cells directly reflects loss of membrane integrity and reduced cell viability following treatment with compounds **4** and **8**.

In preparations examined using an electron microscope, the destructive effects of the tested compounds on selected microorganisms were clearly evident (see Fig. 6).

In control samples, rod-shaped cells (*P. aeruginosa*) and cocci (*S. aureus*) appeared uniformly stained, with well-defined morphology. In contrast, samples treated with the test compounds exhibited irregular staining, distortion of cell shape, and leakage of intracellular contents. Furthermore, the extent of cellular damage increased proportionally with the concentration of the compounds. These ultrastructural observations are fully consistent with the fluorescence microscopy results and support a membrane-targeted mode of action. The combination of membrane permeability assessment (PI staining) and direct visualization of cell morphology (SEM) provides complementary evidence of cell envelope disruption.

In the case of *C. albicans*, optical microscopy was performed using methylene blue dye, which is reduced in living cells. Images shown in Fig. 7 confirm the presence of single stained cells in the control sample, whereas for **4** and **8**, the number of stained (dead) cells exceeded that of unstained (viable) cells. Furthermore, higher concentrations of the compounds caused noticeable cell damage, indicated by cell deformation and dye leakage, and also prevented pseudomycelium formation, as seen in dye-free images.

Collectively, these complementary assays consistently demonstrate that the antimicrobial activity of QASs **4** and **8** is primarily associated with disruption of microbial membrane integrity, leading to leakage of intracellular components, loss of cellular morphology, and ultimately cell death. The convergence of intracellular leakage measurements, propidium iodide fluorescence microscopy, and SEM observations provides evidence at functional, cellular, and ultrastructural levels. Importantly, PI staining is based on the same principle of membrane permeability assessment that is commonly employed in live/dead viability assays and flow cytometric analyses. Therefore, the results obtained using these complementary approaches consistently support a membrane-targeted mode of action characteristic of amphiphilic cationic antimicrobial agents.

The antimicrobial data further support a predominantly chain-length-driven structure–activity relationship. Extension of the cationic alkyl substituent from hexyl to decyl and dodecyl resulted in a pronounced increase in antimicrobial potency, in some cases by several orders of magnitude, whereas exchanging the nicotinate anion for PABA generally produced a smaller, although still measurable, change in MIC

**Table 2**
Effect of selected compounds on the cellular constituents' efflux of indicator microorganisms.

| Microorganism | Optical Density (A = 260) | | | | |
|---|---|---|---|---|---|
| | Control | 4 | | 8 | |
| | | 1000 μg/mL | 1*MIC[a] | 1000 μg/mL | 1*MIC[a] |
| *S. aureus* | 0.004 ± 0.001 | 0.949 ± 0.001 | 0.079 ± 0.001 | >1000 | 0.098 ± 0.001 |
| *P. aeruginosa* | 0.104 ± 0.003 | 0.844 ± 0.001 | 0.274 ± 0.001 | >1000 | 0.454 ± 0.001 |
| *C. albicans* | 0.303 ± 0.001 | >1000 | 0.507 ± 0.002 | >1000 | 0.425 ± 0.001 |

[a] For *S. aureus* MIC = 3.9 μg/mL, for *P. aeruginosa* MIC = 125 μg/mL; for *C. albicans* MIC = 62.5 μg/mL.

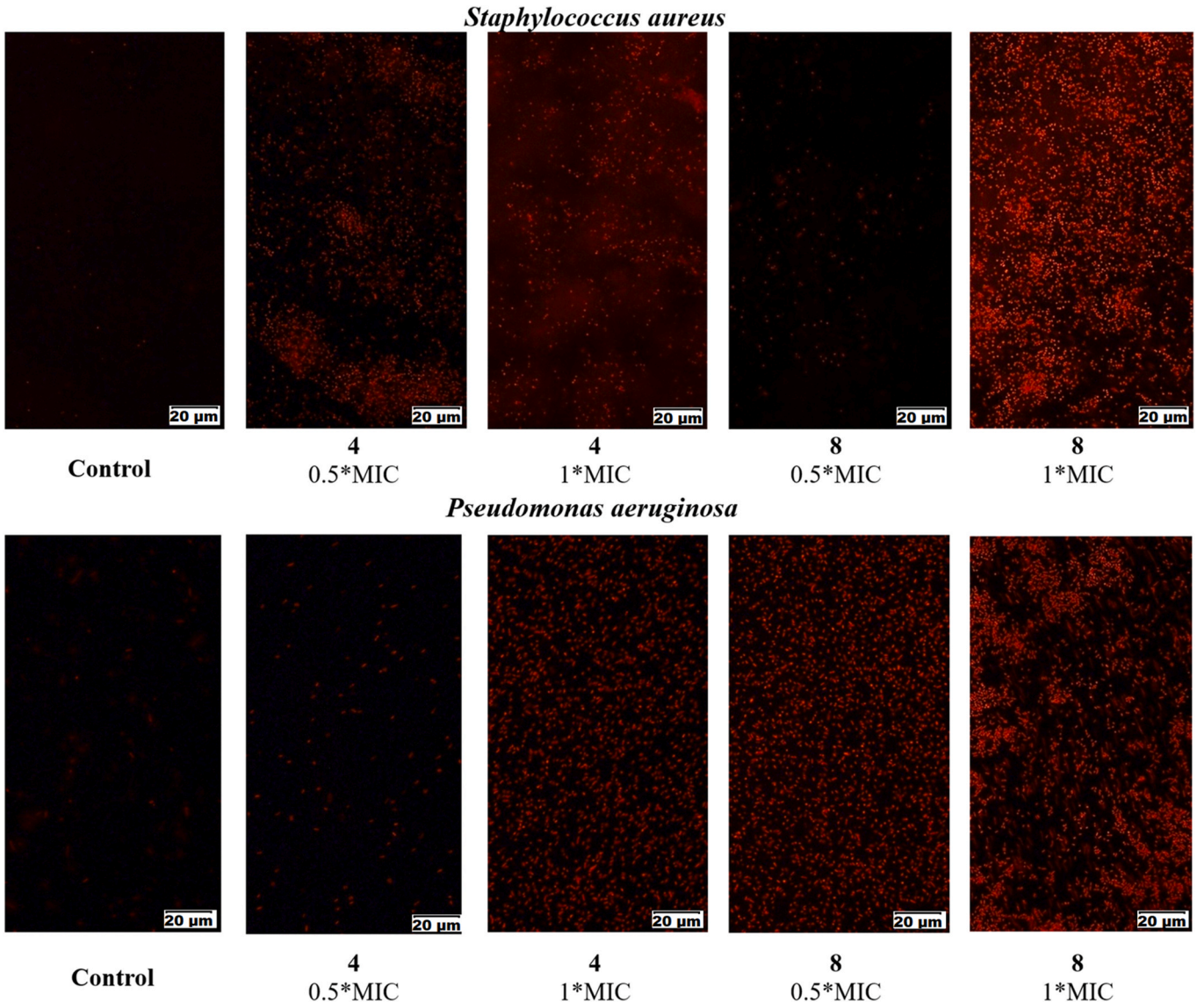


**Fig. 5.** Effects of **4** and **8** on the viability of *S. aureus* and *P. aeruginosa*.

and MBC values. This behavior is consistent with the amphiphilic character of QASs: the permanently charged ammonium group provides electrostatic attraction to the negatively charged microbial surface, while the hydrophobic alkyl chain promotes insertion into and disruption of the lipid membrane. Consequently, increasing chain length enhances membrane interactions and antimicrobial activity, but excessive hydrophobicity may simultaneously increase interactions with mammalian membranes, as observed for compounds **4** and **8** in the cytotoxicity assay.

### *3.5. Solubility of the studied salts (**1**–**8**) and reference systems (**[NA][NIC]** and **[NA][PABA]**) in aqueous solutions of different pH*

Solubility is a key factor in achieving the desired drug concentration in systemic circulation for an optimal pharmacological activity. Water is a versatile solvent and allows the initial classification of substances as well, poorly or very poorly soluble, which is important for formulation development. Poor water solubility is a major challenge in developing formulations for new chemical formulations. Overcoming this issue is crucial, as a drug must be in solution at the absorption site to be effectively absorbed. For orally administered drugs, the gastrointestinal tract represents a critical environment, where the drug initially encounters the acidic conditions of the stomach. The simulated gastric fluid (SGF), with a pH of 1.2, mimics the acidic environment of gastric juice [65]. The physiological pH of blood and most body fluids, including plasma, is equal to approx. 7.4, which is represented by the phosphate-buffered saline (PBS). The compounds analyzed in the course of this work were classified by individual solubility classes according to the standards of the United States Pharmacopoeia (USP) and the British Pharmacopoeia (BP) [31]. The results of solubility measurements in pure distilled water, considered a fundamental physicochemical property of drug candidates, are summarized in Fig. 8 and Table S8 in the Supporting Information. Additional solubility data in SGF and PBS media are presented in Tables S8-S9 in the Supporting Information.

All ionic compounds (**1**–**8**), regardless of the anion, exhibited the highest solubility in water and the lowest in SGF. Notably, the alkyl chain had low impact on solubility, with a clear effect observed only for the dodecyl chain, where the compound typically dropped one solubility category. In general, ionic salts with the *p*-aminobenzoate anion (**5**–**8**) showed better solubility across the tested media, even reaching the 'Very Soluble' category-the highest solubility class. Fascinatingly, compared to the parent acids (NIC and PABA), the solubility of the synthesized QAS increased about 10-fold for **1**-**3** and as much as 1000-fold for **5**-**7**, showing significant improvement. However, such a more pronounced

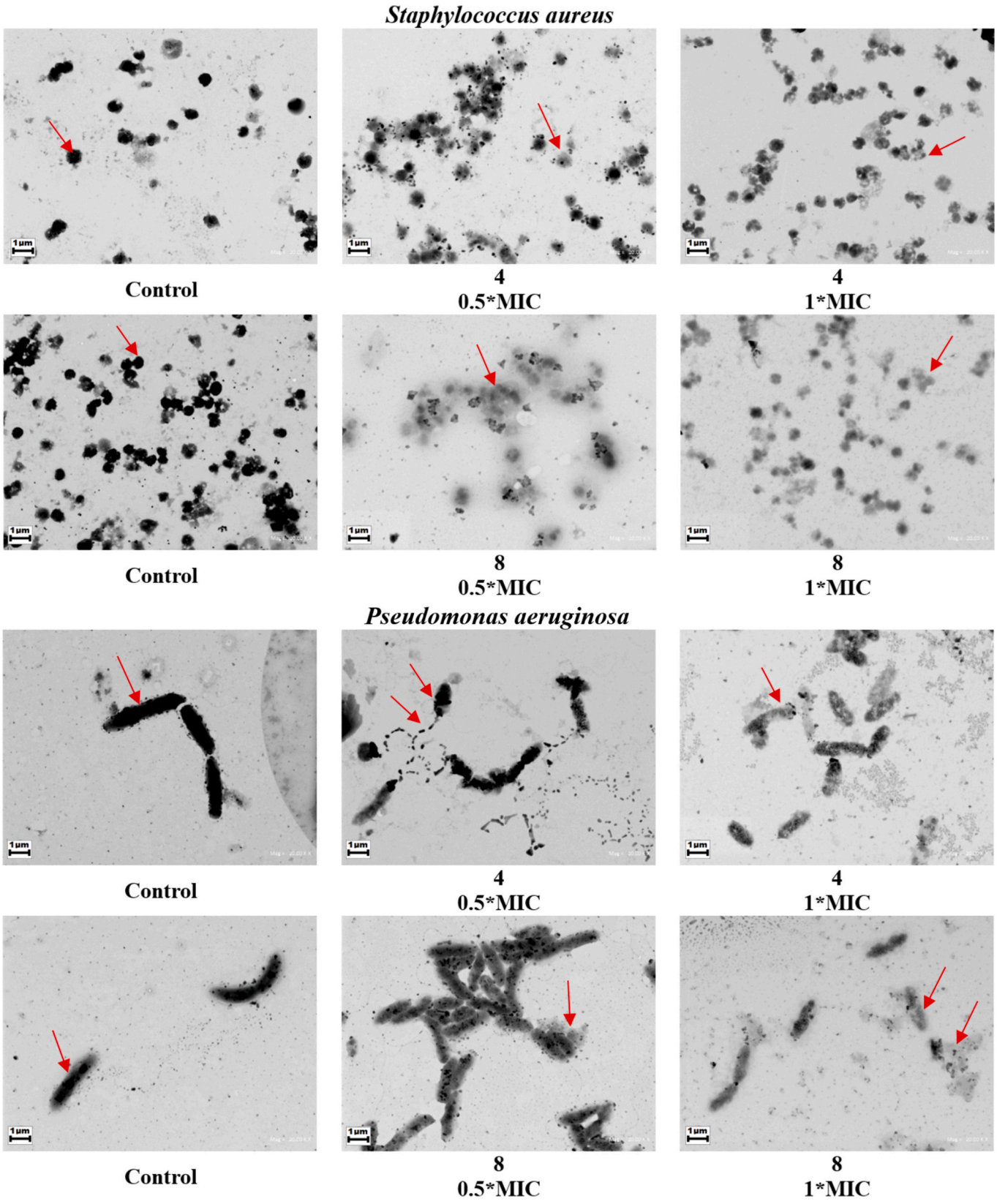


**Fig. 6.** Morphology and viability of *S. aureus and P. aeruginosa* treated with compounds **4** and **8**. The red arrows indicate cells: intact cells with morphology typical of the microorganism in the control sample, and damaged cells in samples exposed to the tested compounds. (For interpretation of the references to color in this figure legend, the reader is referred to the Web version of this article.)

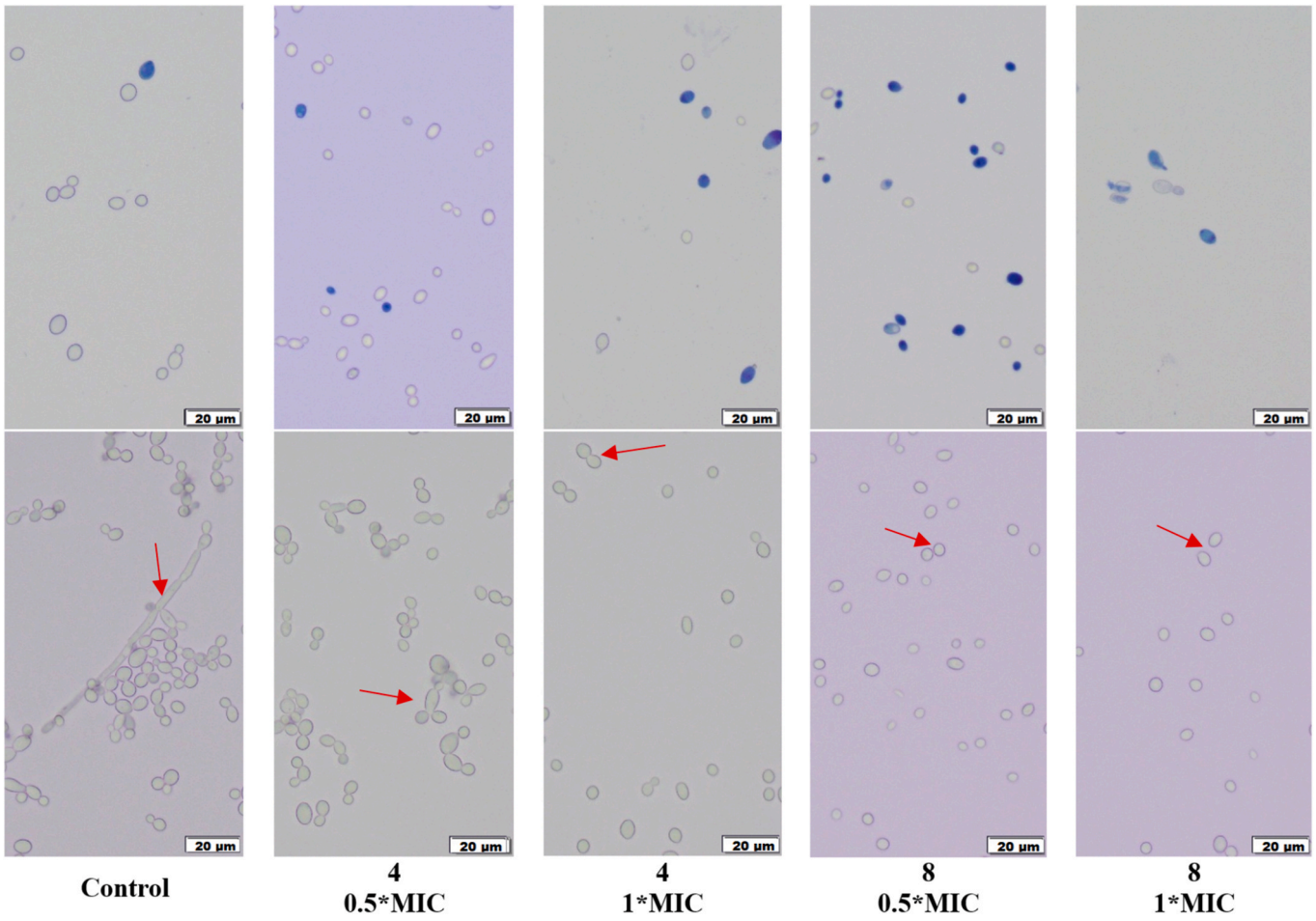


**Fig. 7.** Morphology and viability of *C. albicans* treated with compounds **4** and **8** (upper row - photos with a dye, bottom row - photos without a dye). The red arrows indicate pseudomycelium in the control and deformed cells in the samples exposed to the tested compounds. (For interpretation of the references to color in this figure legend, the reader is referred to the Web version of this article.)

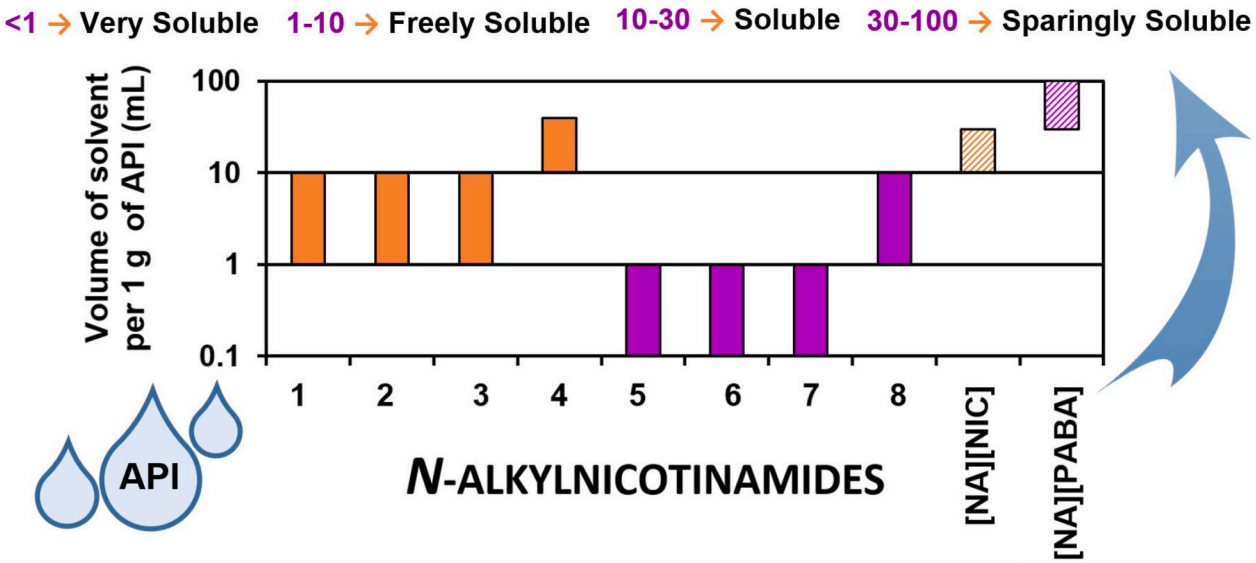


**Fig. 8.** Solubility of *N*-alkylnicotinamide nicotinates (**1-4**), *N*-alkylnicotinamide *p*-aminobenzoates (**5-8**), **[NA] [NIC]** and **[NA] [PABA]** in distilled water.

improvement was not seen for **[NA] [NIC]** and **[NA] [PABA]**, which improved their class by only one category[66,67] Although non-ionic compounds lacked an alkyl chain, typically linked with increased hydrophobicity, they did not follow the expected solubility trends. Therefore, it is clear advantage of QASs that they allow to improve water solubility and bioavailability. Regardless of the solvent, **[NA] [NIC]**

remained 'Soluble', while **[NA] [PABA]** was consistently the least soluble, classified as 'Sparingly Soluble'. The results show that solubility cannot be predicted solely by ionic character or alkyl chain length. They underscore the need for a deeper understanding of the influencing factors that affect it beyond pure hydrophobicity. These findings also solidify the concept of converting inert drug molecules into salts, which manifests in enhancement of APIs overall performance.

These observations indicate that solubility is influenced by a complex interplay of structural factors, where the ionic nature of the compounds plays a dominant role, while alkyl chain length has only a secondary effect, becoming significant mainly for the longest substituents. Moreover, the type of anion further modulates solubility, particularly favoring *p*-aminobenzoate-based systems.

### 3.6. Stability of the studied salts (**4** and **8**) and reference systems (**[NA] [NIC]** and **[NA][PABA]**) in aqueous solutions of different pH

Many regulatory authorities, such as the FDA (ang. *Food and Drug Administration*) or the ICH (ang. *International Council for Harmonisation*), require stability testing of active substances before the release of a new drug on the market [68]. Once absorbed into the bloodstream, the drug must maintain its structural integrity and pharmacological activity to exert its therapeutic effect effectively. Unfortunately, some medicinal substances may undergo hydrolysis, oxidation or other chemical transformations under various conditions [69]. Their degradation products may be toxic, lead to side effects or reduce the effectiveness of the therapy. Through stability studies, potential risks can be identified and the drug formulation adjusted accordingly. In this context, the stability of APIs in aqueous solutions under different pH conditions is considered one of the key factors in the drug design and development process, as it affects both the efficacy and safety of the drug [70,71]. Subsequently, to assess the stabilities of the synthesized QASs, the behavior of and the most promising representatives containing dodecyl group in the cation (**4** and **8**), in different pH environments were evaluated and compared with non-ionic compositions, **[NA] [NIC]** and **[NA] [PABA]**. The results are presented in Fig. 9.

Generally, the tested compounds were established to be most stable in SGF (pH = 1.2). The changes in their spectra were the slightest and at $\lambda_{max}$ = 261-266 nm the absorbance was altered by only approx. 5% after 7 days. Interestingly, salts **4** and **8** were more stable compared to analogous non-ionic systems. This demonstrates that the proposed API-QAS strategy brings additional benefits from the point of view of the stability of a new drug, which should be adequately absorbed in the body to exhibit therapeutic activity.

A study conducted in water provided interesting results, suggesting a trend analogous to that observed in SGF. However, due to the similarity in pH values, only minor differences between tests in water and PBS were expected. Nonetheless, in water, the changes in collected UV spectra were more pronounced in comparison to SGF. In this solvent, salts **4** and **8** were less stable than mixtures, which manifested in notable increase in absorbance at $\lambda_{max}$ and in its vicinity. Notably different effect was observed for tests in PBS (pH = 7.4). It turned out that salts **4** and **8** were multiple times less susceptible to decomposition in comparison to **[NA] [NIC]** and **[NA] [PABA]**, exhibited in substantial changes in UV spectra. In contrast to QASs, their initial peaks were decreasing or increasing by even 75% compared to initial absorbance at $\lambda_{max}$. These significant changes in characteristics of UV spectra suggests that plausibly majority of them was degraded after a week of storage. On the contrary, spectra of salts **4** and **8**, changed only slightly after a week, allowing to conclude that this form is more stable in the utilized pH value. Generally, at pH values mimicking body fluids, the changes in absorbance at $\lambda_{max}$ for QASs remained within 40%, while for **[NA] [NIC]** and **[NA] [PABA]**, the differences reached 75% and 52%, respectively. This unambiguously indicates that organic salts are a more promising drug form compared to their non-ionic counterparts. It should be emphasized that the enhanced stability of QASs compared to non-ionic systems suggests that ionic interactions play a key role in stabilizing the molecular structure, while the presence of long alkyl chains may additionally influence resistance to degradation depending on the pH environment.

Literature data on the stability of DFC-Na at pH 5, 6, 7, and 8 at 45 °C demonstrates that this drug exhibits high stability in applied test conditions. The calculated half-times of decomposition ranged from 107 to 178 days, whereas most stable solution was achieved for pH 5 [72]. Studies focused on the analysis of the hydrolysis rate of NA in the pH range of 0.4–11.3, revealing that its degradation rate depends linearly on its concentration. Notably, NA exhibits the greatest stability and the slowest decomposition in the pH range of 4.5–6. Within this range, its half-life at 89.4 °C was approximated to 1000 days [73]. Interestingly, other report has shown that *N*-hexyl and *N*-octyl alkyl esters of nicotinic acid remain stable in a pH 7.4 buffer at 37 °C, showing no signs of hydrolysis even after five weeks [74]. However, perfluorinated hexyl nicotinic ester and perfluorinated octyl nicotinic ester rapidly degrade at 60 °C, disintegrating within just 45 min [75]. Obviously, the QASs analyzed in the course of this study were less stable than pure NA or some of its analogues. However, considering the proposed oral route of administration, they should exhibit sufficient stability. Combined with their high therapeutic and multifunctional activity, which allows for the use of very low doses, these compounds emerge as highly promising new APIs.

### 3.7. Cytotoxicity to human intestinal cells

Cytotoxicity assessment is a crucial early step in the preclinical development of compounds intended for oral administration, as the intestinal epithelium represents an important biological barrier encountered after ingestion [76]. Local toxicity at the level of the small intestine can disrupt epithelial integrity, impair drug absorption, and limit its therapeutic use, regardless of systemic safety. This issue is particularly relevant for amphiphilic and cationic compounds, such as QASs, which are known to interact with biological membranes in a structure-dependent manner [77]. Cytotoxicity was primarily evaluated based on the viability of intestinal epithelial cells exposed to the analyzed compounds at concentrations ranging from 1 to 100 μg/mL, which are generally considered physiologically relevant and achievable *in vivo*. In this context, most of the compounds tested were well tolerated by human intestinal epithelial cells.

As was shown in Fig. 10, both non-alkylated salts, **[NA] [NIC]** and **[NA] [PABA]**, as well as QAS derivatives with short alkyl chains (**1**, **2**, **5**, and **6**), did not cause a decrease in intestinal cell viability. The relative cell viability reminded above 93% across the entire tested concentration range, up to 100 μg/mL, indicating a lack of cytotoxic potential under conditions relevant to intestinal exposure. A slight reduction in cell viability was noted in cultures treated with compounds **3** and **7**, with calculated $IC_{10}$ values of 45.9 and 65.7 μg/mL, respectively. The $IC_{50}$ values for these compounds exceeded the investigated concentration window (see Table S10 in Supporting Information). In contrast, derivatives bearing the longest alkyl chains (**4** and **8**) within the physiologically relevant range induced pronounced cytotoxic effects with $IC_{50}$ values of 20.1 and 15.0 μg/mL, respectively. These compounds elicited lethal effects ($IC_{90}$) at concentrations below 35 μg/mL, suggesting strong interactions with the cell membrane. Overall, a clear structure–activity relationship was observed: increasing alkyl chain length led to progressively enhanced cytotoxicity. This trend mirrors the antimicrobial activity profile and supports a membrane-mediated mechanism of action. Importantly, the nature of the counterion exerted only a minor influence on cytotoxicity; for corresponding homologues, PABA salts displayed slightly lower $IC_{50}$ values than their nicotinate analogues, although this effect was marginal compared to that of alkyl chain elongation.

Noteworthy, the reference QAS, benzalkonium chloride (BAC), widely used in pharmaceutical formulations (listed in Table S1 in

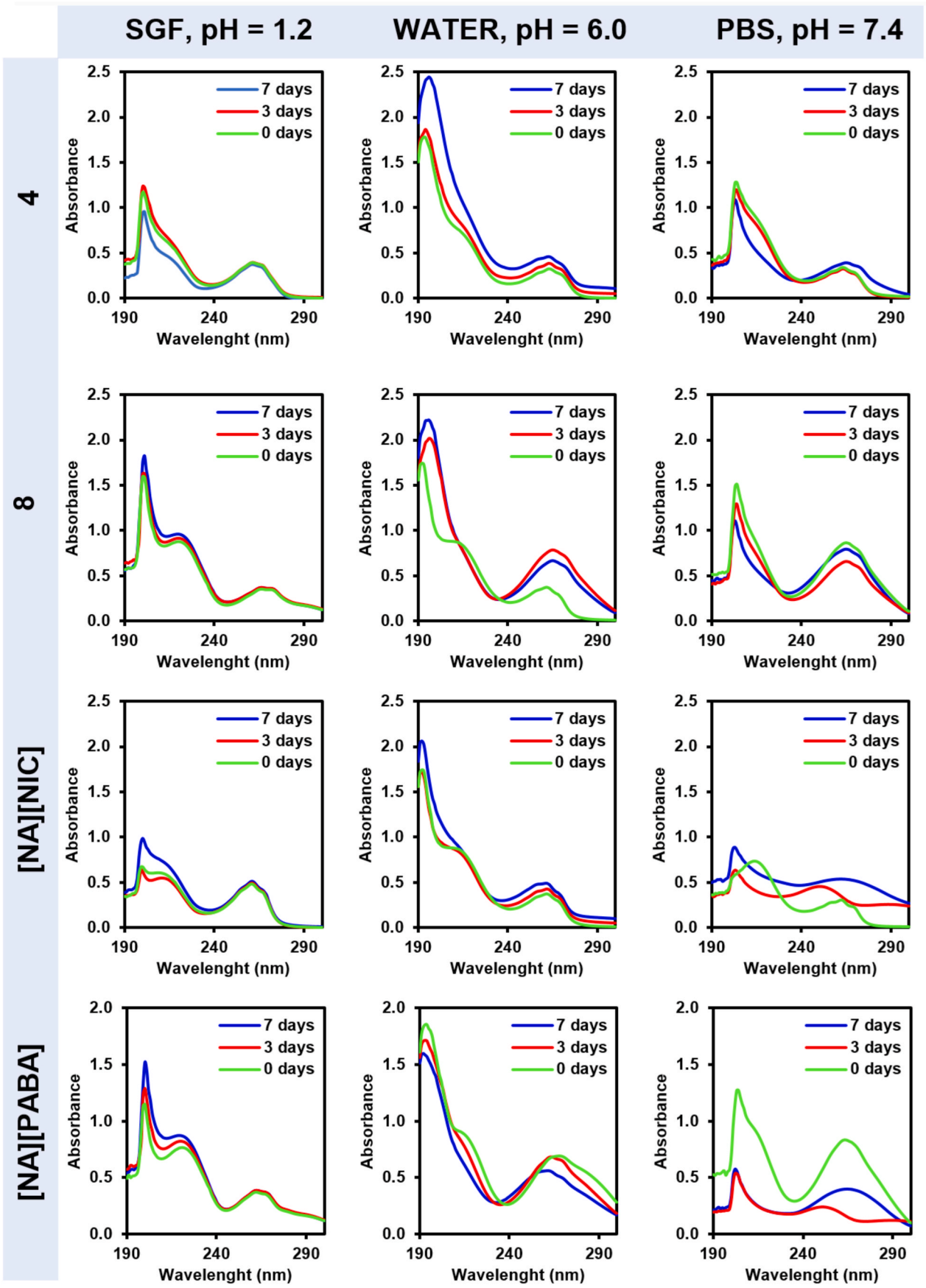


**Fig. 9.** Stability in aqueous solutions of different pH for *N*-dodecylnicotinamide nicotinate (**4**), *N*-dodecylnicotinamide *p*-aminobenzoate (**8**), **[NA] [NIC]** and **[NA] [PABA]** .

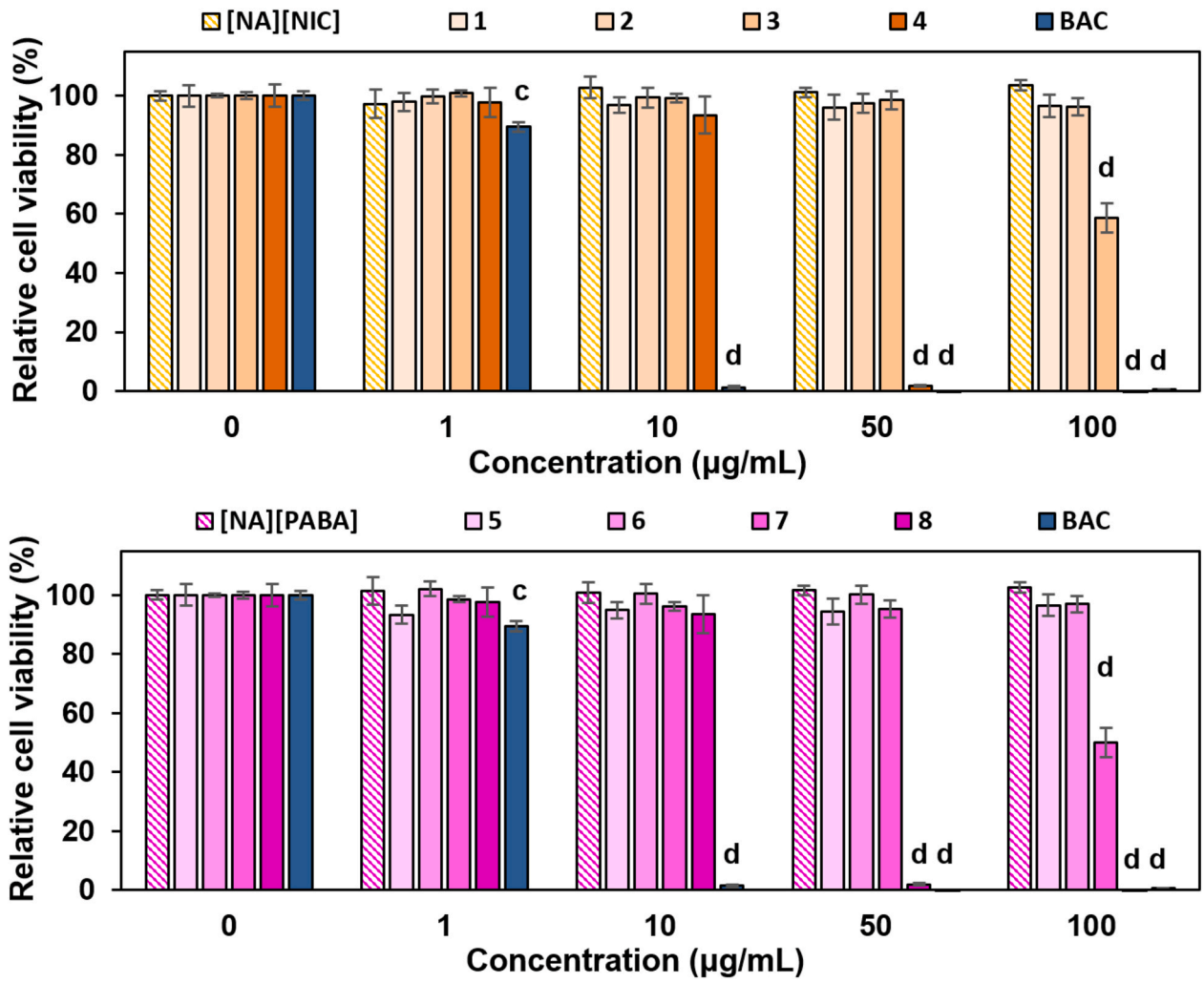


**Fig. 10.** Effect of *N*-alkylnicotinamide nicotinates (**1**-**4**) and *p*-aminobenzoates (**5**-**8**), **[NA] [NIC]**, **[NA] [PABA]** on the viability of human normal small intestinal cells (HIEC-6) in comparison to commercial pharmaceutical (**BAC**).

Supporting Information), exhibited pronounced cytotoxicity toward HIEC-6 cells, with an $IC_{50}$ value of 1.97 μg/mL. Comparable values have been reported for cetylpyridinium chloride (CPC), with $IC_{50}$ ranging from 0.66 to 1.04 μg/mL in hepatocellular carcinoma cells and 2.55–3.16 μg/mL in normal cells [78]. Importantly, even the most cytotoxic nicotinamide-based derivatives (**4** and **8**) were approximately one order of magnitude less toxic than BAC, whereas the short- and medium-chain analogues exhibited $IC_{50}$ values several orders of magnitude higher, indicating substantially lower cytotoxicity. This comparison clearly demonstrates the markedly improved safety profile of the investigated salts relative to classical quaternary ammonium surfactants. While the increased cytotoxicity observed for compounds **4** and **8** suggests that systemic (oral) administration may be limited for derivatives bearing a dodecyl alkyl chain, these compounds may still be considered promising candidates for topical antimicrobial applications, analogous to current BAC- or CPC-containing products.

Overall, cytotoxicity was found to be predominantly determined by alkyl chain length, with longer chains leading to increased membrane interaction and reduced cell viability, whereas the effect of the counterion remains relatively minor. This confirms that hydrophobicity-driven membrane disruption is the main factor governing cytotoxic effects. Interestingly, although both antimicrobial activity and cytotoxicity increased with alkyl-chain length, the vitamin-derived ionic framework maintained a substantially lower cytotoxicity than the conventional QAS reference BAC, indicating that structural modification of the cationic head group can improve the activity–toxicity balance even when amphiphilic character is retained.

To further assess the relationship between cytotoxicity and antimicrobial activity, the therapeutic index (TI) was calculated as the ratio of the cytotoxic $IC_{50}$ value to the corresponding MIC value. The calculated TI values for compounds **1–8** and the reference compounds are presented in Table S11 (Supporting Information). For the shortest-chain derivatives **1** and **5**, bearing a hexyl chain, the TI values could not be precisely determined for most microorganisms because their antimicrobial activity was observed above the highest concentration tested, resulting only in upper-limit TI values (*e.g.*, <5.18 and < 6.42 for compounds **1** and **5**, respectively). For the octyl derivatives **2** and **6**, antimicrobial activity was observed within the tested concentration range, and the calculated TI values were generally in the range of approximately 0.7–3, depending on the microorganism. For example, compound **2** showed TI values of 1.48 against *S. aureus* and 2.97 against *C. neoformans*, whereas compound **6** reached values of 1.56 and 3.12 against these microorganisms, respectively. A more pronounced microorganism-dependent variation was observed for salts comprising decyl group (**3** and **7**). In general, Gram-positive bacteria exhibited more favorable TI values than Gram-negative bacteria. Moreover, the nicotinate derivative **3** generally showed higher TI values than its PABA analogue **7**; for example, against *S. aureus*, the TI values were 2.47 and 1.62 for **3** and **7**, respectively. A similar trend was observed for **4** and **8**, whereas nicotinate (**4**) generally exhibited more favorable TI values

than the corresponding PABA salt (**8**). The derivatives with the longest (dodecyl) chain showed the largest number of TI values above 1, with values reaching 5.16 for compound **4** against *S. aureus* and *B. subtilis*, while compound **8** reached a TI of 3.84 against *S. aureus* and *C. neoformans*. Importantly, the TI analysis provides additional quantitative support for the proposed structure–activity relationship, as the longer-chain derivatives generally combined stronger antimicrobial activity with an increased cytotoxic burden, while the nature of the counterion produced a more moderate effect. Thus, the biological profile of these QASs is determined by a balance between alkyl-chain-dependent membrane activity and counterion-dependent modulation of molecular and physicochemical properties.

### 3.8. Ecotoxicity towards aquatic life

Designing drugs that are safe for both the treated organism and the environment is essential, as it supports sustainable development and ensures that medical progress does not harm ecological health. Species of *Artemia franciscana*, known as indicator of aquatic toxicity, can be used to assess the environmental impact of compounds, offering valuable insights into potential risks to aquatic ecosystems. This approach not only enhances our understanding of biological activity but also ensures that new drugs are environmentally safe [21]. Ecotoxicity data toward *A. franciscana* for the prepared compounds are listed in Fig. 11.

The determined $EC_{50}$ values clearly express the benign nature of almost all analyzed salts. Among tested group, QAS **1** has the shortest (hexyl) chain within cation, and as such it is the less toxic and classified as 'Relatively Harmless'. On the contrary, the greatest toxicity was noted for salt **4**, comprising the longest dodecyl chain, being categorized as 'Slightly Toxic.' This observation suggests that within the group with the nicotinate anion (**1–4**) there is an explicit relationship between the alkyl chain length and the increase of the toxic effect toward *A. franciscana*. However, all other compounds, were classified as 'Practically Nontoxic'; hence, for homologous series containing PABA anion (**5–8**), an analogous tendency does not occur. Noteworthy, the collected results revealed the crucial benefit originating from the QASs concept in comparison to non-ionic composition, wherein the incorporation of relatively long alkyl into nicotinamide leads to enhancement of potential therapeutic effects with simultaneous low influence on toxicity toward model aquatic crustacean. Toxicity studies on analogous ionic salts composed of *N*-alkylnicotinamide cations and salicylate anions revealed a similar trend: the salt with a long alkyl chain (dodecyl) was classified as 'Slightly Toxic'. Interestingly, the salt with a shorter alkyl chain (hexyl) is within a lower toxicity category, being labeled as 'Practically Nontoxic', emphasizing the significant influence of the anion on the biological activity of the tested salts. Furthermore, the cocrystal of nicotinamide and salicylic acid, similarly to **[NA] [NIC]** and **[NA] [PABA]**, was also classified as 'Practically Nontoxic' [21].

| Compound | $EC_{50}$ [mg $L^{-1}$] | Class |
|---|---|---|
| **1** | >1000 | Relatively Harmless |
| **2** | 187.7 | Practically Nontoxic |
| **3** | 168.5 | Practically Nontoxic |
| **4** | 97.2 | Slightly Toxic |
| **5** | 677.8 | Practically Nontoxic |
| **6** | 342.9 | Practically Nontoxic |
| **7** | 316.7 | Practically Nontoxic |
| **8** | 123.1 | Practically Nontoxic |
| **[NA][NIC]** | 593.9 | Practically Nontoxic |
| **[NA][PABA]** | 744.4 | Practically Nontoxic |

**Fig. 11.** Ecotoxicity toward *A. franciscana* for *N*-alkylnicotinamide nicotinates (**1-4**), *N*-alkylnicotinamide *p*-aminobenzoates (**5-8**), **[NA] [NIC]** and **[NA] [PABA]**. Class according to acute toxicity rating scale by Fish and Wildlife Service.

Intriguingly, ecotoxicity was influenced primarily by alkyl chain length in nicotinate-based salts, while this trend is less pronounced for *p*-aminobenzoate analogues, highlighting the role of the counterion in modulating environmental impact. Importantly, the incorporation of alkyl chains enhances biological activity without a proportional increase in ecotoxicity.

### 3.9. Bioavailability and toxicity of ionic therapeutic substances - opportunities and limitations

In addition to a drug's therapeutic efficacy, its ability to reach its target sites of action is crucial. To better predict the fate of drugs in the body and assess their actual absorption, *in silico* studies were conducted on the substances analyzed. The bioavailability score was 0.55 and 0.56 for salts **1**–**8** and non-ionic substances (**[NA] [NIC]** and **[NA] [PABA]**), respectively. These values are considered optimal and indicate very good absorption, comparable to that of diclofenac sodium or the widely used sodium salt of ibuprofen [79]. The permeation of ionic drugs in the body after oral administration is a subject of broad consideration. It should be emphasized that the absorption of ionic substances in the intestine is primarily mediated by transport proteins, which enable their movement both along and against the concentration gradient. Although the process is not yet fully understood, it is known that anion transport is facilitated by OATP (Organic Anion Transporting Polypeptide) proteins, while cation transport is mediated by OCT (Organic Cation Transporter) proteins. Anions and zwitterions have dedicated transporters that facilitate their passage into the bloodstream, whereas cations may face difficulties due to the lack of an efficient transporter, limiting their bioavailability [80]. Although the mechanisms are becoming better understood, the transport of ionic compounds, especially cationic ones, still requires further research to fully understand their role and impact on drug bioavailability. In addition to oral administration itself, API-ILs have also been used to enhance the uptake of poorly water-soluble drugs. These ILs provided up to a 20-fold increase in drug absorption compared to analogous suspension formulations administered to rats, while remaining non-toxic and non-irritating [81].

The medical applicability of QASs represents a complex, multifactorial challenge, driven by their broad-spectrum activity. Although they exhibit pronounced biological effect, particularly antibacterial, their efficacy is often accompanied by cytotoxicity and safety concerns, which may limit the application potential of the obtained experimental results. In particular, long-chain QASs derivatives are often characterized by significant cytotoxicity, which practically eliminates them from the group of potential drug candidates. It is therefore crucial to seek an optimal balance between antimicrobial efficacy and safety. Specifically, the described products with shorter alkyl chains exhibit excellent anti-inflammatory activity and reduced cytotoxicity risk, albeit at the expense of diminished antimicrobial effects. Intriguingly, elongation of the alkyl chain reduces the effective concentration of the anti-inflammatory effect and introduces additional antimicrobial activity. This tunable multifunctionality allows for the design of derivatives with the most desirable properties regarding, both biological activity and safety. The optimization of not only chemical structure but also key parameters such as compound concentration, exposure duration, and route of administration represents a promising strategy for the successful application of QASs that exhibit sufficient therapeutic efficacy while minimizing adverse effects. For this reason, the concept of API-QASs still continues to be a focus of intensive research in pharmacology.

New vitamin B derivatives have a high potential for diverse applications. Their strong anti-inflammatory and bactericidal properties make them suitable not only for oral drug formulations but also for topical therapeutic preparations. Notable mention refers to benzalkonium chloride (BAC), an ingredient found in many commercial antibacterial preparations used for treating ear, eye, or upper respiratory tract infections. Their typical concentrations used in pharmaceutical formulations range from 0.01% to 0.13%, therefore considering that the MIC values observed in our study were as low as 3.9 mg/L (0.00039%), the required effective concentration of analyzed compounds would fall well below the upper thresholds typically applied in drug products. This therefore proves that by controlling the concentration appropriately, we can obtain effective active substances that merge high activity with an acceptable safety profile. It further supports translational relevance of QASs, indicating that antimicrobial efficacy can be achieved at concentrations far lower than those commonly employed in existing medical formulations. Altogether, approach presented in this work emphasizes not only efficacy but also biocompatibility and formulation feasibility, supporting the potential of vitamin B derivatives for further development in medical applications. Additionally, their cytotoxic properties, including QASs with dodecyl substituent (**4** and **8**), are multiple times weaker compared to that of BAC. In effect, they plausibly will be much safer after administration, which makes them excellent replacement not only to BAC, but also many other surface active QASs.

Importantly, even in cases where the compounds comprising shorter alkyl chains (**1**, **2**, **5** and **6**) did not demonstrate pronounced antibacterial activity, they exhibited another therapeutically valuable feature, which is anti-inflammatory activity. This property, often overlooked, is highly desirable in the treatment of infections. A key advantage of our compounds lies in the fact that their relatively lower antibacterial activity, initially perceived as a potential drawback, is in fact compensated by their significant anti-inflammatory potential. We have demonstrated that the obtained compounds have high anti-inflammatory activity comparable or even superior to the commonly used anti-inflammatory drug - diclofenac. Additionally, a dual-functionality, exhibited particularly by QASs with longer alkyls (**3**, **4**, **7** and **8**), broadens their applicability and positions them as promising candidates not only for antimicrobial therapies but also for applications in inflammatory or wound-healing contexts, where modulation of the immune response is equally critical.

Among the various factors used to assess the toxicity and therapeutic limitations of ionic compounds, hemolytic activity is of particular importance, especially for cationic amphiphilic agents such as QASs, due to their potential ability to disrupt erythrocyte membranes. This effect is strongly structure-dependent and generally correlates with increasing alkyl chain length and hydrophobicity, which simultaneously enhance antimicrobial activity. Experimental studies on QAS-based systems have shown that compounds with log $K_{OW}$ higher than 2 exhibit increased hemolytic activity. This is likely due to their stronger membrane-disruptive effects, while more hydrophilic analogues remain largely hemocompatible [82]. Interestingly, QASs investigated in this study display low lipophilicity (log $K_{OW}$ from −1.73 to 0.35), suggesting a limited intrinsic hemolytic potential. For comparison, widely used QASs such as benzalkonium chloride (BAC) exhibit substantially higher lipophilicity (log $K_{OW} \approx$ 2.2–3.9) and are known to induce hemolysis at very low concentrations (complete hemolysis observed at ~0.002–0.003%). Despite this, BAC remains broadly used in pharmaceutical formulations, demonstrating that hemolytic activity is strongly dose-dependent and can be effectively mitigated through appropriate formulation strategies [83]. Moreover, the synthesized derives of vitamin B exhibit significantly lower hydrophobicity and reduced surface-active properties compared to BAC, which may further contribute to their improved safety profile [84]. Similarly, QAS-based copolymeric systems have been reported to exhibit relatively low hemolysis (<10–25% at 50 μg/mL), with $HC_{50}$ values exceeding 50 μg/mL, indicating that appropriate tuning of alkyl chain length allows for achieving a balance between antimicrobial efficacy and hemocompatibility [85]. Among fluorinated ILs hemolysis was generally observed only at concentrations close to or exceeding the CMC, supporting the feasibility of these systems for drug delivery applications within controlled concentration ranges. Noteworthy, 1-methyl-3-octylimidazolium perfluoromethanesulfonate uniquely combined antibacterial activity with minimal hemolysis (≤3.15% at active concentrations), clearly distinguishing it from the other compounds [86]. Other API-ILs, based on the ibuprofenate anion and cholinium or imidazolium cations, remained hemocompatible even at concentrations exceeding the maximum plasma concentration of ibuprofen [87]. Therefore, although the physicochemical profile of the investigated compounds suggests a low hemolytic risk, comprehensive evaluation under physiologically relevant conditions remains an important direction for future studies.

## 4. Conclusions

Novel QASs with forms of vitamin B in both the cation and anion were synthesized, characterized and investigated as novel APIs. These QASs were designed to be multifunctional (anti-inflammatory and antimicrobial) drugs. Mixtures and cocrystals of the starting materials were investigated as well for comparison purposes. Most of the QASs showed better potential anti-inflammatory activity, with up to 54% inhibition of egg albumin denaturation (**6**), outperforming diclofenac sodium at its maximum plasma concentration. *In silico* molecular docking studies consistently demonstrated that elongation of the alkyl chain in QASs cations enhances COX-2 binding affinity, with the longest chains exhibiting stronger and more complete engagement than diclofenac, highlighting their potential as novel anti-inflammatory agents. The antimicrobial activity of ionic salts was significantly enhanced, up to 250-fold compared to their non-ionic analogues, particularly for derivatives with decyl (**3**, **7**) and dodecyl (**4**, **8**) alkyl chains. Compounds with longest alkyls (**4**, **8**) also showed exceptional antibiofilm activity, achieving 100% inhibition of *S. aureus* and *P. aeruginosa* strains. Biological action of **4** and **8** has been primarily associated with disruption of microbial membrane integrity leading to leakage of intracellular components. Solubility and stability studies confirmed the favorable pharmaceutical properties of the ionic forms over the entire pH range. The measured log $K_{OW}$ values ranged from approximately −1.73 to 0.35, with the salt with nicotinate anion (**1**–**4**) showing higher lipophilicity than their counterparts with the anion derived from *p*-aminobenzoic acid (**5**–**8**). This set if results along with the calculated bioavailability (0.55–0.56) suggests promising oral absorption, comparable to conventional drugs. Cytotoxicity analysis using human normal small intestinal cells (HIEC-6) revealed that salts with hexyl and octyl chains (**1**, **2**, **5** and **6**) up to 100 μg/mL did not affect cell viability, similarly to their non-alkylated analogues, indicating non-cytotoxic potential within physiologically relevant concentrations. In contrast, dodecyl derivatives (**4** and **8**) reduced cell viability in the physiologically achievable range, indicating enhanced membrane interactions typical of amphiphilic QASs. Nevertheless, these compounds remained markedly less cytotoxic than benzalkonium chloride, highlighting their promise as alternative antimicrobial agents. While systemic use of long-chain analogues may be limited, they appear particularly suitable for topical applications. Ecotoxicity tests using model organisms (*Artemia franciscana*) showed that almost all tested salts are potentially benign for the aquatic ecosystems.

The promising data obtained in the present study justify further extensive investigations, including both *in vitro* and *in vivo* studies, to confirm the observed antimicrobial and anti-inflammatory activities and to evaluate the pharmacokinetic properties, bioavailability, and systemic safety of the tested compounds in a physiological context.

## CRediT authorship contribution statement

**Adriana Olejniczak:** Writing – original draft, Visualization,

Resources, Methodology, Investigation, Funding acquisition, Formal analysis, Data curation, Conceptualization. **Daniela Gwiazdowska:** Writing – review & editing, Supervision, Methodology, Formal analysis, Data curation. **Krzysztof Juś:** Writing – review & editing, Methodology, Investigation, Formal analysis. **Anna Olejnik:** Writing – review & editing, Methodology, Investigation, Formal analysis, Data curation. **Mara G. Freire:** Writing – review & editing, Validation. **Michał Niemczak:** Writing – review & editing, Validation, Supervision, Resources, Project administration, Funding acquisition.

## Declaration of competing interests

The authors declare the following financial interests/personal relationships which may be considered as potential competing interests: Michal Niemczak reports financial support was provided by Ministry of Science and Higher Education. Adriana Olejniczak reports financial support was provided by Ministry of Science and Higher Education. If there are other authors, they declare that they have no known competing financial interests or personal relationships that could have appeared to influence the work reported in this paper.

## Acknowledgment

This research was funded by the Ministry of Science and Higher Education as a subsidy to Poznan University of Technology in Poland (0912/SBAD/2504) and by the 'PhDBoost' Program for doctoral students of the Doctoral School of Poznan University of Technology (in 2024) from the University's subsidy financed from the funds of Ministry of Science and Higher Education (0912/SPHD/2521).

## Appendix A. Supplementary data

Supplementary data to this article can be found online at https://doi.org/10.1016/j.jddst.2026.108853.

## Data availability

Data will be made available on request.

## References

[1] M. Miethke, M. Pieroni, T. Weber, M. Brönstrup, P. Hammann, L. Halby, P. B. Arimondo, P. Glaser, B. Aigle, H.B. Bode, R. Moreira, Y. Li, A. Luzhetskyy, M. H. Medema, J.-L. Pernodet, M. Stadler, J.R. Tormo, O. Genilloud, A.W. Truman, K. J. Weissman, E. Takano, S. Sabatini, E. Stegmann, H. Brötz-Oesterhelt, W. Wohlleben, M. Seemann, M. Empting, A.K.H. Hirsch, B. Loretz, C.-M. Lehr, A. Titz, J. Herrmann, T. Jaeger, S. Alt, T. Hesterkamp, M. Winterhalter, A. Schiefer, K. Pfarr, A. Hoerauf, H. Graz, M. Graz, M. Lindvall, S. Ramurthy, A. Karlén, M. van Dongen, H. Petkovic, A. Keller, F. Peyrane, S. Donadio, L. Fraisse, L.J.V. Piddock, I. H. Gilbert, H.E. Moser, R. Müller, Towards the sustainable discovery and development of new antibiotics, Nat. Rev. Chem 5 (2021) 726–749, https://doi.org/10.1038/s41570-021-00313-1.

[2] O.E. Okpala, J. Rondevaldova, L. Kokoska, Anti-inflammatory drugs as potential antimicrobial agents: a review, Front. Pharmacol. 16 (2025) 1–19, https://doi.org/10.3389/fphar.2025.1557333.

[3] J. Feder-Kubis, A. Wirwis, M. Policht, J. Singh, K.-H. Kim, Principles and practice of greener ionic liquid–nanoparticles biosystem, Green Chem. 26 (2024) 3072–3124, https://doi.org/10.1039/D3GC04387H.

[4] B. Gaida, A. Brzęczek-Szafran, Insights into the properties and potential applications of renewable carbohydrate-based ionic liquids: a review, Molecules (25) (2020) 3285, https://doi.org/10.3390/molecules25143285.

[5] J.L. Shamshina, R.D. Rogers, Ionic liquids: new forms of active pharmaceutical ingredients with unique, tunable properties, Chem. Rev. 123 (2023) 11894–11953, https://doi.org/10.1021/acs.chemrev.3c00384.

[6] S.S. Bharate, Recent developments in pharmaceutical salts: FDA approvals from 2015 to 2019, Drug Discov. Today 26 (2021) 384–398, https://doi.org/10.1016/j.drudis.2020.11.016.

[7] K.S. Egorova, E.G. Gordeev, V.P. Ananikov, Biological activity of ionic liquids and their application in pharmaceutics and medicine, Chem. Rev. 117 (2017) 7132–7189, https://doi.org/10.1021/acs.chemrev.6b00562.

[8] B. Zhou, D. Teng, J. Li, Y. Zhang, M. Qi, M. Hong, G.-B. Ren, Development of a gliclazide ionic liquid and its mesoporous silica particles: an effective formulation strategy to improve oral absorption properties, RSC Adv. 12 (2022) 1062–1076, https://doi.org/10.1039/D1RA07499G.

[9] S. Celik, A. Ali Tugrul, A. Sevim, A.E. Ozel, Synthesis, molecular docking and ADMET study of ionic liquid as anticancer inhibitors of DNA and COX-2, TOPII enzymes, J. Biomol. Struct. Dyn. 38 (2020) 1354–1364, https://doi.org/10.1080/07391102.2019.1604263.

[10] R.M. Moshikur, M.K. Ali, R. Wakabayashi, M. Moniruzzaman, M. Goto, Methotrexate-based ionic liquid as a potent anticancer drug for oral delivery: in vivo pharmacokinetics, biodistribution, and antitumor efficacy, Int. J. Pharm. 608 (2021) 121129, https://doi.org/10.1016/j.ijpharm.2021.121129.

[11] E. Hasan, A. Syed Nawazish, B. Zarina, B. Sabira, A. Sundus, S. Afshan, B. S. Siddiqui, An efficient synthesis of O- and N- alkyl derivatives of 4-aminobenzoic acid and evaluation of their anticancer properties, Nat. Prod. Res. 38 (2024) 2220–2230, https://doi.org/10.1080/14786419.2023.2169916.

[12] C. Munteanu, S.M. Mârza, I. Papuc, The immunomodulatory effects of vitamins in cancer, Front. Immunol. 15 (2024), https://doi.org/10.1016/j.jpha.2013.09.003.

[13] A. Kluczyk, T. Popek, T. Kiyota, P. de Macedo, P. Stefanowicz, C. Lazar, Y. Konishi, Drug evolution: p-aminobenzoic acid as a building block, Curr. Med. Chem. 9 (2002) 1871–1892, https://doi.org/10.2174/0929867023368872.

[14] S.I. Akberova, New biological properties of p-Aminobenzoic acid, Biol. Bull. Russ. Acad. Sci. 29 (2002) 390–393, https://doi.org/10.1023/A:1016871219882.

[15] T. Dang, I.S. Nizamov, R.Z. Salikhov, L.R. Sabirzyanova, V.V. Vorobev, T. I. Burganova, M.M. Shaidoullina, E.S. Batyeva, R.A. Cherkasov, T.I. Abdullin, Synthesis and characterization of pyridoxine, nicotine and nicotinamide salts of dithiophosphoric acids as antibacterial agents against resistant wound infection, Bioorg. Med. Chem. 27 (2019) 100–109, https://doi.org/10.1016/j.bmc.2018.11.017.

[16] E.M. Ahmed, N.A. Khalil, E. Ramadan, T. Tharwat, M.A. Ali, Z. Mahmoud, Synthesis and biological evaluation of new nicotinic acid derivatives as potential anti-inflammatory agents with enhanced gastric safety profile, Bioorg. Chem. 144 (2024) 107136, https://doi.org/10.1016/j.bioorg.2024.107136.

[17] M. Lappas, M. Permezel, The anti-inflammatory and antioxidative effects of nicotinamide, a vitamin B3 derivative, are elicited by FoxO3 in human gestational tissues: implications for preterm birth, J. Nutr. Biochem. 22 (2011) 1195–1201, https://doi.org/10.1016/j.jnutbio.2010.10.009.

[18] S.J. Bachofer, Micelle formation of tetradecyltrimethylammonium X-benzoate surfactants: benzoate counterion substituent effects, J. Surfactants Deterg. 27 (2024) 259–267, https://doi.org/10.1080/07391102.2019.1604263.

[19] A. Caković, D. Ćoćić, M. Živanović, N. Janković, N. Milivojević, M. Delibašić, M. Kostić, I. Radojević, M. Grujović, K.G. Marković, O.R. Klisurić, M. Vraneš, J. Bogojeski, Enhancing bioactivity of N,N,N-Chelating Rhodium(III) complexes with ionic liquids: toward targeted cancer therapy, J. Med. Chem. 67 (2024) 13349–13362, https://doi.org/10.1021/acs.jmedchem.4c01220.

[20] G. Chantereau, M. Sharma, A. Abednejad, C. Vilela, E.M. Costa, M. Veiga, F. Antunes, M.M. Pintado, G. Sèbe, V. Coma, M.G. Freire, C.S.R. Freire, A.J. D. Silvestre, Bacterial nanocellulose membranes loaded with vitamin B-based ionic liquids for dermal care applications, J. Mol. Liq. 302 (2020) 112547, https://doi.org/10.1016/j.molliq.2020.112547.

[21] A. Olejniczak, W. Stachowiak, D. Ziental, J. Długaszewska, T. Rzemieniecki, M. Wysokowski, T. Jesionowski, M. Niemczak, Unraveling the potential of vitamin B3-Derived salts with a salicylate anion as dermal active agents for acne treatment, Mol. Pharm. 21 (2024) 4634–4647, https://doi.org/10.1021/acs.molpharmaceut.4c00543.

[22] W. Stachowiak, D.K. Kaczmarek, T. Rzemieniecki, M. Niemczak, Sustainable design of new ionic forms of vitamin B3 and their utilization as plant protection agents, J. Agric. Food Chem. 70 (2022) 8222–8232, https://doi.org/10.1021/acs.jafc.2c01807.

[23] OECD Publishing, OECD, Test No. 123: Partition Coefficient (1-Octanol/Water): Slow-Stirring Method, OECD Guidelines for the Testing of Chemicals, Section 1, 1-17, OECD Publishing, Paris, OECD Guidel. Test. Chem. (2022), https://doi.org/10.1787/9789264015845-en.

[24] P. Chaiya, S. Senarat, T. Phaechamud, W. Narakornwit, In vitro anti-inflammatory activity using thermally inhibiting protein denaturation of egg albumin and antimicrobial activities of some organic solvents, Mater. Today Proc. 65 (2022) 2290–2295, https://doi.org/10.1016/j.matpr.2022.04.916.

[25] D.K. Kaczmarek, T. Rzemieniecki, D. Gwiazdowska, T. Kleiber, T. Praczyk, J. Pernak, Choline-based ionic liquids as adjuvants in pesticide formulation, J. Mol. Liq. 327 (2021) 114792, https://doi.org/10.1016/j.molliq.2020.114792.

[26] D. Gwiazdowska, P.A. Uwineza, S. Frąk, K. Juś, K. Marchwińska, R. Gwiazdowski, A. Waśkiewicz, Antioxidant, antimicrobial and antibiofilm properties of Glechoma hederacea extracts obtained by supercritical fluid extraction, using different extraction conditions, Appl. Sci. (12) (2022) 3572, https://doi.org/10.3390/app12073572.

[27] M. Somrani, M.-C. Inglés, H. Debbabi, F. Abidi, A. Palop, Garlic, onion, and cinnamon essential oil anti-biofilms' effect against Listeria monocytogenes, Foods (9) (2020) 567, https://doi.org/10.3390/foods9050567.

[28] S. Paul, R.C. Dubey, D.K. Maheswari, S.C. Kang, Trachyspermum ammi (L.) fruit essential oil influencing on membrane permeability and surface characteristics in inhibiting food-borne pathogens, Food Control 22 (2011) 725–731, https://doi.org/10.1016/j.foodcont.2010.11.003.

[29] J. Zhang, S. Ma, S. Du, S. Chen, H. Sun, Antifungal activity of thymol and carvacrol against postharvest pathogens Botrytis cinerea, J. Food Sci. Technol. 56 (2019) 2611–2620, https://doi.org/10.1007/s13197-019-03747-0.

[30] N. Bou-Chacra, K.J.C. Melo, I.A.C. Morales, E.S. Stippler, F. Kesisoglou, M. Yazdanian, R. Löbenberg, Evolution of choice of solubility and dissolution

media after two decades of biopharmaceutical classification system, AAPS J. 19 (2017) 989–1001, https://doi.org/10.1208/s12248-017-0085-5.
[31] K.T. Savjani, A.K. Gajjar, J.K. Savjani, Drug solubility: importance and enhancement techniques, ISRN Pharm 2012 (2012) 195727, https://doi.org/10.5402/2012/195727.
[32] M. Aslam, G. Pandey, N. Deshwal, A. Kumar, K. Kumari, I. Bahadur, P. Singh, F. Mohammad, A. Abdullah Soleiman, Study the solubility of pharmaceutical ingredients and their eutectic mixtures: an in-depth density functional theory and molecular dynamics simulations approaches, J. Mol. Liq. 397 (2024) 124070, https://doi.org/10.1016/j.molliq.2024.124070.
[33] A. Becker, API co-crystals – trends in CMC-Related aspects of pharmaceutical development beyond solubility, Drug Discov. Today 28 (2023) 103527, https://doi.org/10.1016/j.drudis.2023.103527.
[34] M. Niemczak, Ł. Sobiech, M. Grzanka, Iodosulfuron-methyl-based herbicidal ionic liquids comprising alkyl betainate cation as novel active ingredients with reduced environmental impact and excellent efficacy, J. Agric. Food Chem. 68 (2020) 13661–13671, https://doi.org/10.1021/acs.jafc.0c05850.
[35] M. Niemczak, T. Rzemieniecki, Ł. Sobiech, G. Skrzypczak, T. Praczyk, J. Pernak, Influence of the alkyl chain length on the physicochemical properties and biological activity in a homologous series of dichlorprop-based herbicidal ionic liquids, J. Mol. Liq. 276 (2019) 431–440, https://doi.org/10.1016/j.molliq.2018.12.013.
[36] L. Zhu, L. Lu, S. Wang, J. Wu, J. Shi, T. Yan, C. Xie, Q. Li, M. Hu, Z. Liu, Chapter 11 - oral absorption basics: pathways and physicochemical and biological factors affecting absorption, in: Y. Qiu, Y. Chen, G.G.Z. Zhang, L. Yu, R.V.B.T. Mantri (Eds.), D.S.O.D.F, Academic Press, Boston, 2017, pp. 297–329, https://doi.org/10.1016/B978-0-12-802447-8.00011-X. Second E.
[37] S. Trohalaki, R. Pachter, Prediction of melting points for ionic liquids. QSAR comb, Sci. 24 (2005) 485–490, https://doi.org/10.1002/qsar.200430927.
[38] D. Tzeli, I.D. Petsalakis, G. Theodorakopoulos, D. Ajami, J. Rebek Jr, Theoretical study of free and encapsulated carboxylic acid and amide dimers, Int. J. Quant. Chem. 113 (2013) 734–739, https://doi.org/10.1002/qua.24062.
[39] D. Tzeli, G. Theodorakopoulos, I.D. Petsalakis, D. Ajami, J. Rebek, Theoretical study of hydrogen bonding in homodimers and heterodimers of amide, boronic acid, and carboxylic acid, free and in encapsulation complexes, J. Am. Chem. Soc. 133 (2011) 16977–16985, https://doi.org/10.1021/ja206555d.
[40] A. Buanz, T.J. Prior, J.C. Burley, B.T. Raimi-Abraham, R Telford, M. Hart, C. C. Seaton, P.J. Davies, I.J. Scowen, S. Gaisford, G.R. Williams, Thermal Behavior of Benzoic Acid/Isonicotinamide Binary Cocrystals, Cryst. Growth Des. 15 (2015) 3249–3256, https://doi.org/10.1021/acs.cgd.5b00351.
[41] V.R. Hathwar, R. Pal, T.N. Guru Row, Charge density analysis of crystals of nicotinamide with salicylic acid and oxalic acid: an insight into the salt to cocrystal continuum, Cryst. Growth Des. 10 (2010) 3306–3310, https://doi.org/10.1021/cg100457r.
[42] L. Di, E.H. Kerns, Profiling drug-like properties in discovery research, Curr. Opin. Chem. Biol. 7 (2003) 402–408, https://doi.org/10.1016/S1367-5931(03)00055-3.
[43] G.-M. Cárdenas-Youngs, J.-L. Beltrán, Dissociation constants and octanol–water partition equilibria for several fluoroquinolones, J. Chem. Eng. Data 60 (2015) 3327–3332, https://doi.org/10.1021/acs.jced.5b00556.
[44] S.D. Chitnis, Y. Han, M. Yamaguchi, S. Mita, R. Zhao, G. Sunkara, K. Kulmatycki, Population pharmacokinetic modeling and noncompartmental analysis demonstrated bioequivalence between metformin component of metformin/vildagliptin fixed-dose combination products and metformin immediate-release tablet sourced from various countries, Clin. Pharmacol. Drug Dev. 5 (2016) 40–51, https://doi.org/10.1002/cpdd.191.
[45] T. Ingram, U. Richter, T. Mehling, I. Smirnova, Modelling of pH dependent n-octanol/water partition coefficients of ionizable pharmaceuticals, Fluid Phase Equilib. 305 (2011) 197–203, https://doi.org/10.1016/j.fluid.2011.04.006.
[46] A. Kumar, A. Jindal, Cytotoxicity and bioavailability assessment from micellar system based thiamine-phospholipid complexes, J. Mol. Liq. 407 (2024) 125177, https://doi.org/10.1016/j.molliq.2024.125177.
[47] V. Sarveiya, J.F. Templeton, H.A.E. Benson, Ion-pairs of ibuprofen: increased membrane diffusion, J. Pharm. Pharmacol. 56 (2004) 717–724, https://doi.org/10.1211/0022357023448.
[48] L. Chen, H. Deng, H. Cui, J. Fang, Z. Zuo, J. Deng, Y. Li, X. Wang, L. Zhao, Inflammatory responses and inflammation-associated diseases in organs, Oncotarget 9 (2018) 7204–7218, https://doi.org/10.18632/oncotarget.23208.
[49] E. Kuchar, M. Karlikowska-Skwarnik, D. Wawrzuta, Anti-inflammatory therapy of infections, in: N.B.T. Rezaei (Ed.), E. of I. and I., Elsevier, Oxford, 2022, pp. 791–797, https://doi.org/10.1016/B978-0-12-818731-9.00181-6.
[50] J.D. Villeda-González, J.L. Gómez-Olivares, L.A. Baiza-Gutman, L. Manuel-Apolinar, L. Damasio-Santana, C. Millán-Pacheco, S. Ángeles-Mejía, M.C. Cortés-Ginez, M. Cruz-López, C.J. Vidal-Moreno, M. Díaz-Flores, Nicotinamide reduces inflammation and oxidative stress via the cholinergic system in fructose-induced metabolic syndrome in rats, Life Sci. 250 (2020) 117585, https://doi.org/10.1016/j.lfs.2020.117585.
[51] J.V. Willis, M.J. Kendall, R.M. Flinn, D.P. Thornhill, P.G. Welling, The pharmacokinetics of diclofenac sodium following intravenous and oral administration, Eur. J. Clin. Pharmacol. 16 (1979) 405–410, https://doi.org/10.1007/BF00568201.
[52] F.M. Walocko, A.E. Eber, J.E. Keri, M.A. Al-Harbi, K. Nouri, The role of nicotinamide in acne treatment, Dermatol. Ther. 30 (2017) e12481, https://doi.org/10.1111/dth.12481.
[53] E. Holzhäuser, C. Albrecht, Q. Zhou, A. Buttler, M.R. Preusch, E. Blessing, H. A. Katus, F. Bea, Nicotinic acid has anti-atherogenic and anti-inflammatory properties on advanced atherosclerotic lesions independent of its lipid-modifying capabilities, J. Cardiovasc. Pharmacol. 57 (2011) 447–454, https://doi.org/10.1097/FJC.0b013e31820dc1db.
[54] J.E. Digby, F. Martinez, A. Jefferson, N. Ruparelia, J. Chai, M. Wamil, D.R. Greaves, R.P. Choudhury, Anti-inflammatory effects of nicotinic acid in human monocytes are mediated by GPR109A dependent mechanisms, Arterioscler. Thromb. Vasc. Biol. 32 (2012) 669–676, https://doi.org/10.1161/ATVBAHA.111.241836.
[55] M. Bhatia, A. Kumar, V. Verma, S. Devi, Development of ketoprofen-p-aminobenzoic acid co-crystal: formulation, characterization, optimization, and evaluation, Med. Chem. Res. 30 (2021) 2090–2102, https://doi.org/10.1007/s00044-021-02794-7.
[56] X. Wu, W. Lan, Q. Chen, Y. Dong, J. Liu, W. Peng, Inferring LncRNA-disease associations based on graph autoencoder matrix completion, Comput. Biol. Chem. 87 (2020) 107282, https://doi.org/10.1016/j.compbiolchem.2020.107282.
[57] B. Brycki, A. Szulc, Gemini Alkyldeoxy-D-Glucitolammonium salts as modern surfactants and microbiocides: synthesis, antimicrobial and surface activity, biodegradation, PLoS One 9 (2014) e84936, https://doi.org/10.1371/journal.pone.0084936.
[58] Y. Hu, Y. Xing, H. Yue, T. Chen, Y. Diao, W. Wei, S. Zhang, Ionic liquids revolutionizing biomedicine: recent advances and emerging opportunities, Chem. Soc. Rev. 52 (2023) 7262–7293, https://doi.org/10.1039/D3CS00510K.
[59] J.S. Katz, Y. Tan, K. Kuppannan, Y. Song, D.J. Brennan, T. Young, L. Yao, S. Jordan, Amino-acid-incorporating nonionic surfactants for stabilization of protein pharmaceuticals, ACS Biomater. Sci. Eng. 2 (2016) 1093–1096, https://doi.org/10.1021/acsbiomaterials.6b00245.
[60] D.C. Kaat, D. Nicolas, D.B. Katrijn, P. Annelies, K. Soña, G. Evelien, V. Natalie, M. Jan, V. Patrick, T. Karin, Oral administration of the broad-spectrum antibiofilm compound toremifene inhibits Candida albicans and Staphylococcus aureus biofilm formation in vivo, Antimicrob. Agents Chemother. 58 (2014) 7606–7610, https://doi.org/10.1128/aac.03869-14.
[61] S. Sharma, J. Mohler, S.D. Mahajan, S.A. Schwartz, L. Bruggemann, R. Aalinkeel, Microbial biofilm: a review on formation, infection, antibiotic resistance, control measures, and innovative treatment, Microorganisms (11) (2023) 1614, https://doi.org/10.3390/microorganisms11061614.
[62] S. Mishra, A. Gupta, V. Upadhye, S.C. Singh, R.P. Sinha, D.-P. Häder, Therapeutic strategies against biofilm infections, Life (13) (2023) 172, https://doi.org/10.3390/life13010172.
[63] J.F. González, M.M. Hahn, J.S. Gunn, Chronic biofilm-based infections: skewing of the immune response, Pathog. Dis. 76 (2018) fty023, https://doi.org/10.1093/femspd/fty023.
[64] S.D. Cox, J.E. Gustafson, C.M. Mann, J.L. Markham, Y.C. Liew, R.P. Hartland, H. C. Bell, J.R. Warmington, S.G. Wyllie, Tea tree oil causes K+ leakage and inhibits respiration in Escherichia coli, Lett. Appl. Microbiol. 26 (1998) 355–358, https://doi.org/10.1046/j.1472-765x.1998.00348.x.
[65] J. Bevernage, B. Hens, J. Brouwers, J. Tack, P. Annaert, P. Augustijns, Supersaturation in human gastric fluids, Eur. J. Pharm. Biopharm. 81 (2012) 184–189, https://doi.org/10.1016/j.ejpb.2012.01.017.
[66] M.H. Abraham, W.E. Acree, On the solubility of nicotinic acid and isonicotinic acid in water and organic solvents, J. Chem. Thermodyn. 61 (2013) 74–78, https://doi.org/10.1016/j.jct.2013.01.024.
[67] T.D. Turner, D.M.C. Corzo, D. Toroz, A. Curtis, M.M. Dos Santos, R.B. Hammond, X. Lai, K.J. Roberts, The influence of solution environment on the nucleation kinetics and crystallisability of para-aminobenzoic acid, Phys. Chem. Chem. Phys. 18 (2016) 27507–27520, https://doi.org/10.1039/C6CP04320H.
[68] M. Blessy, R.D. Patel, P.N. Prajapati, Y.K. Agrawal, Development of forced degradation and stability indicating studies of drugs—A review, J. Pharm. Anal. 4 (2014) 159–165, https://doi.org/10.1016/j.jpha.2013.09.003.
[69] A. Gabrič, Ž. Hodnik, S. Pajk, Oxidation of drugs during drug product development: problems and solutions, Pharmaceutics (14) (2022) 325, https://doi.org/10.3390/pharmaceutics14020325.
[70] S. Acharya, B.R. Guru, Prednisolone encapsulated PLGA nanoparticles: characterization, cytotoxicity, and anti-inflammatory activity on C6 glial cells, J. Appl. Pharmaceut. Sci. 10 (2020) 14–21, https://doi.org/10.7324/japs.2020.104003.
[71] P. Khadka, J. Ro, H. Kim, I. Kim, J.T. Kim, H. Kim, J.M. Cho, G. Yun, J. Lee, Pharmaceutical particle technologies: an approach to improve drug solubility, dissolution and bioavailability, Asian J. Pharm. Sci. 9 (2014) 304–316, https://doi.org/10.1016/j.ajps.2014.05.005.
[72] R. Chadha, N. Kashid, D.V.S. Jain, Kinetics of degradation of diclofenac sodium in aqueous solution determined by a calorimetric method, Pharmazie 58 (2003) 631–635.
[73] P. Finholt, T. Higuchi, Rate studies on the hydrolysis of niacinamide, J. Pharmaceut. Sci. 51 (1962) 655–661, https://doi.org/10.1002/jps.2600510710.
[74] G.N. Wernly-Chung, J.M. Mayer, T.-K. Anna, B. Testa, Structure-reactivity relationships in the chemical hydrolysis of prodrug esters of nicotinic acid, Int. J. Pharm. 63 (1990) 129–134, https://doi.org/10.1016/0378-5173(90)90162-W.
[75] C.-H. Hsu, M. Jay, P.M. Bummer, H.-J. Lehmler, Chemical stability of esters of nicotinic acid intended for pulmonary administration by liquid ventilation, Pharm. Res. 20 (2003) 918–925, https://doi.org/10.1023/A:1023899505837.
[76] B. Ziemba, Advances in cytotoxicity testing: from in vitro assays to in silico models, Int. J. Mol. Sci. (26) (2025) 11202, https://doi.org/10.3390/ijms262211202.
[77] S.S. Moosavi, A.R. Zolghadr, Effect of Quaternary ammonium surfactants on biomembranes using molecular dynamics simulation, RSC Adv. 13 (2023) 33175–33186, https://doi.org/10.1039/D3RA05030K.
[78] K. Cai, Y. Fang, Y. Zhang, J. Liu, Q. Ye, L. Ding, X. Cai, Cetylpyridinium chloride inhibits hepatocellular carcinoma growth and metastasis through regulating

epithelial-mesenchymal transition and apoptosis, PLoS One 19 (2024) e0310391, https://doi.org/10.1371/journal.pone.0310391.
[79] N.H. Metwally, G.H. Elgemeie, A.R. Abdelrazek, S.M. Eldaly, Synthesis, antibacterial evaluation and in silico studies of novel 2-(benzo[d]thiazol-2-yl)-N-arylacetamides and their derivatives as potential DHFR inhibitors, BMC Chem. 19 (2025) 29, https://doi.org/10.1186/s13065-025-01386-5.
[80] W.R. Proctor, X. Ming, D. Bourdet, T. (Kevin) Han, R.S. Everett, D.R. Thakker, Why does the intestine lack basolateral efflux transporters for cationic compounds? A provocative hypothesis, J. Pharmaceut. Sci. 105 (2016) 484–496, https://doi.org/10.1016/j.xphs.2015.11.040.
[81] Y. Sahbaz, H.D. Williams, T.-H. Nguyen, J. Saunders, L. Ford, S.A. Charman, P. J. Scammells, C.J.H. Porter, Transformation of poorly water-soluble drugs into lipophilic ionic liquids enhances oral drug exposure from lipid based formulations, Mol. Pharm. 12 (2015) 1980–1991, https://doi.org/10.1021/mp500790t.
[82] P.T. Phuong, S. Oliver, J. He, E.H.H. Wong, R.T. Mathers, C. Boyer, Effect of hydrophobic groups on antimicrobial and hemolytic activity: developing a predictive tool for ternary antimicrobial polymers, Biomacromolecules 21 (2020) 5241–5255, https://doi.org/10.1021/acs.biomac.0c01320.
[83] G. Dehghan-Noudeh, M. Housaindokht, B.S. Fazly Bazzaz, Isolation, characterization, and investigation of surface and hemolytic activities of a lipopeptide biosurfactant produced by *Bacillus subtilis* ATCC 6633, J. Microbiol. 43 (2005) 272–276, https://doi.org/10.1007/BF02928154.
[84] G.N. Mathioudakis, A. Soto Beobide, G. Bokias, P.G. Koutsoukos, G.A. Voyiatzis, Surface-enhanced raman scattering as a tool to study cationic surfactants exhibiting low critical micelle concentration, J. Raman Spectrosc. 51 (2020) 452–460, https://doi.org/10.1002/jrs.5798.
[85] R. Tejero, D. López, F. López-Fabal, J.L. Gómez-Garcés, M. Fernández-García, High efficiency antimicrobial thiazolium and triazolium side-chain polymethacrylates obtained by controlled alkylation of the corresponding azole derivatives, Biomacromolecules 16 (2015) 1844–1854, https://doi.org/10.1021/acs.biomac.5b00427.
[86] N.S.M. Vieira, A.L.S. Oliveira, J.M.M. Araújo, M.M. Gaspar, A.B. Pereiro, Ecotoxicity and hemolytic activity of fluorinated ionic liquids, Sustainable Chemistry 2 (2021) 115–126, https://doi.org/10.3390/suschem2010008.
[87] J.C. Bastos, N.S.M. Vieira, M.M. Gaspar, A.B. Pereiro, J.M.M. Araújo, Human cytotoxicity, hemolytic activity, anti-inflammatory activity and aqueous solubility of ibuprofen-based ionic liquids, Sustainable Chemistry 3 (2022) 358–375, https://doi.org/10.3390/suschem3030023.